

Supplementary Material

Antibody Dynamics of Severe and Non-Severe Patients with COVID-19

Fernanda Ordoñez-Jiménez¹, Rodolfo Blanco-Rodríguez¹, Alexis Erich S. Almocera², Gustavo Chinney-Herrera¹ and Esteban Hernández-Vargas^{1,3}

(1) Instituto de Matemáticas, Universidad Nacional Autónoma de México, Boulevard Juriquilla 3001, Querétaro, Qro., 76230, México.

(2) Division of Physical Sciences and Mathematics, College of Arts and Sciences, University of the Philippines Visayas, Philippines.

(3) Frankfurt Institute for Advanced Studies, Frankfurt am Main, Germany.

Corresponding: esteban@im.unam.mx

A. Bifurcation analysis

We seek an equilibrium point with virus, denoted E^* . To obtain a working expression for E^* , we introduce

$$\overline{w_M} = \frac{\overline{r_M}}{\overline{q} + \delta_M}, \quad \overline{w_G} = \frac{\overline{r_q} \overline{w_M}}{\delta_G}^2.$$

Let us introduce the function

$$f(x, \lambda) = \left(\frac{\overline{c_G} \overline{w_G}}{\overline{c_T}} \right) [x^2 - (\hat{y} + x_G^*) x] + \left(\frac{\lambda + \overline{c_T}}{\overline{c_T}} \right), \quad (25)$$

$$\mathcal{H}_0(x, \lambda) = 1 - \frac{1}{f(x, \lambda)} = \frac{f(x, \lambda) - 1}{f(x, \lambda)}, \quad (26)$$

where

$$x_G^* = (\overline{w_M})^{-1} + (\overline{w_G})^{-1}, \quad \hat{y} = \frac{\overline{c_M} \overline{w_M} + 1}{\overline{c_G} \overline{w_G}}.$$

Writing $E^* = (x^*, y^*, z^*, w_M^*, w_G^*)$ where $x^* > 0$, we establish that E^* is a function of x^* .

Theorem 2. A necessary condition for E^* to exist is $\lambda + \overline{c_T} > 0$. Under this condition, E^* takes the form

$$E^* = (x^*, f(x^*, \lambda), x^*, \overline{w_M} x^*, \overline{w_G} x^*(x_G^* - x^*)) \quad (27)$$

where x^* satisfies

$$\mathcal{H}(x^*, \overline{K_T}) = \mu \mathcal{H}_0(x^*, \lambda), \quad \mu := \overline{\delta_T}/\overline{r_T}. \quad (28)$$

Proof. Eqs. (16)-(20) provide the following equations:

$$0 = \lambda + \overline{c_T} - x^* - \overline{c_T}y^* - \overline{c_M}w_M^* - \overline{c_G}w_G^*, \quad (29)$$

$$0 = \overline{\delta_T} + \overline{r_T}y^* \mathcal{H}(x^*, \overline{K_T}) - \overline{\delta_T}y^*, \quad (30)$$

$$0 = (\overline{\tau_B})^{-1}(x^* - z^*), \quad (31)$$

$$0 = \overline{r_M}z^* - (\overline{q} + \overline{\delta_M})w_M^*, \quad (32)$$

$$0 = \overline{r_q}w_M^*(1 - w_M^*) + \overline{\delta_G}(z^* - w_G^*), \quad (33)$$

with $\lambda + \overline{c_T} = 1 - \bar{c}$. If E^* exists, then we get

$$0 = \lambda + \overline{c_T} - x^* - \overline{c_T}y^* - \overline{c_M}w_M^* - \overline{c_G}w_G^* < \lambda + \overline{c_T}$$

from Eq. 29. Therefore, it is necessary that $\lambda + \overline{c_T} > 0$ for E^* to exist.

Proceeding with the condition $\lambda + \overline{c_T} > 0$, we get $z^* = x^*$ from Eq (31). Now, we can rewrite Eqs. (32) and (33) as

$$0 = \overline{w_M}(\overline{q} + \overline{\delta_M})x^* - (\overline{q} + \overline{\delta_M})w_M^*, \quad (34)$$

$$0 = \overline{w_G}\overline{\delta_G}w_M^*(1 - w_M^*) + \overline{w_M}^2\overline{\delta_G}(z^* - w_G^*). \quad (35)$$

Eq. (34) yields

$$w_M^* = \overline{w_M}x^*. \quad (36)$$

Substituting this result into Eq. (35), we obtain

$$0 = \overline{w_G}\overline{\delta_G}\overline{w_M}x^*(1 - \overline{w_M}x^*) + \overline{w_M}^2\overline{\delta_G}(x^* - w_G^*),$$

$$0 = \overline{w_G}x^*(1 - \overline{w_M}x^*) + \overline{w_M}(x^* - w_G^*),$$

$$w_G^* = \overline{w_G}x^*((\overline{w_M})^{-1} - x^*) + x^*,$$

$$\begin{aligned} w_G^* &= \overline{w}_G x^* ((\overline{w}_M)^{-1} + (\overline{w}_G)^{-1} - x^*), \\ w_G^* &= \overline{w}_G x^* (x_G^* - x^*). \end{aligned} \tag{37}$$

From Eq. (29) we have

$$\overline{c}_T y^* = \lambda + \overline{c}_T - x^* - \overline{c}_M w_M^* - \overline{c}_G w_G^*. \tag{38}$$

Substituting Eqs. (37) and (36) into Eq. (38), we get

$$\begin{aligned} \overline{c}_T y^* &= \lambda + \overline{c}_T - x^* - \overline{c}_M \overline{w}_M x^* - \overline{c}_G \overline{w}_G x^* (x_G^* - x^*), \\ \overline{c}_T y^* &= \overline{c}_G \overline{w}_G (x^*)^2 - (1 + \overline{c}_M \overline{w}_M + \overline{c}_G \overline{w}_G x_G^*) (x^*) + \lambda + \overline{c}_T, \\ \overline{c}_T y^* &= \overline{c}_G \overline{w}_G [(x^*)^2 - (\hat{y} + x_G^*) (x^*)] + \lambda + \overline{c}_T. \end{aligned}$$

The last equation is equivalent to $y^* = f(x^*, \lambda)$. Therefore, E^* takes the form in Eq. (27). Moreover, taking $y^* = f(x^*, \lambda)$ in Eq. (30) yields:

$$\begin{aligned} 0 &= \overline{\delta}_T + \overline{r}_T f(x^*, \lambda) \mathcal{H}(x^*, \overline{K}_T) - \overline{\delta}_T f(x^*, \lambda), \\ \mathcal{H}(x^*, \overline{K}_T) &= \frac{\overline{\delta}_T f(x^*, \lambda) - \overline{\delta}_T}{\overline{r}_T f(x^*, \lambda)}, \end{aligned}$$

which is Eq. (28). \square

Theorem 3. Assume that $\lambda + \overline{c}_T > 0$ and let $\mathcal{H}_G^* := \mathcal{H}(x_G^*, \overline{K}_T)$. Let \mathcal{I} be the set of all x such that

- $0 < x \leq x_G^*$,
- $f(x, \lambda) > 1$, and
- either $\mu \leq \mathcal{H}_G^*$ or $f(x, \lambda) \leq \frac{\mu}{\mu - \mathcal{H}_G^*}$.

Then every virus-positive equilibrium point E^* has the viral load $x^* \in \mathcal{I}$.

Proof. Eq. (27) in Theorem 2 requires that $f(x^*, \lambda) > 0$ and $0 < x^* \leq x_G^*$. Since $\mathcal{H}(x, \lambda)$ increases over positive values of x , we have

$$\begin{aligned} 0 < \mathcal{H}(x^*, \lambda) &\leq \mathcal{H}_G^* \\ \iff 0 < \mathcal{H}_0(x^*, \lambda) &\leq \frac{\mathcal{H}_G^*}{\mu} \end{aligned} \tag{by Eq. (28)}$$

$$\begin{aligned} \Leftrightarrow 0 &< \frac{f(x^*, \lambda) - 1}{f(x^*, \lambda)} \leq \frac{\mathcal{H}_G^*}{\mu} && \text{by Eq. (26)} \\ \Leftrightarrow 1 &< f(x^*, \lambda) \leq 1 + \frac{\mathcal{H}_G^*}{\mu} f(x^*, \lambda) \end{aligned}$$

The last inequality is equivalent to

$$f(x^*, \lambda) \left[1 - \frac{\mathcal{H}_G^*}{\mu} \right] \leq 1 < f(x^*, \lambda),$$

or

$$f(x^*, \lambda) > 1, \text{ and either } \mu \leq \mathcal{H}_G^* \text{ or } f(x^*, \lambda) \leq \frac{\mu}{\mu - \mathcal{H}_G^*}.$$

Therefore, $x \in \mathcal{I}$. □

The set \mathcal{I} in Theorem 3 locates all possible values of the positive viral load x^* at E^* . Note that this set may take different forms according to λ and μ . Both quantities put bound restrictions on $f(x, \lambda)$ as follows:

- The parameter λ restricts $f(x, \lambda)$ with $f(x, \lambda) > 1$, which is needed for both $y^* > 0$ and $\mathcal{H}_0(x^*) > 0$.
- If $\mu > \mathcal{H}_G^*$, then μ puts an additional restriction: $f(x, \lambda) \leq \mu/(\mu - \mathcal{H}_G^*)$.

To determine these forms, we collect some properties of f as a quadratic function in x restricted to the interval $(0, x_G^*]$.

1. We have $f(\hat{y}, \lambda) = f(x_G^*, \lambda) < f(0, \lambda)$ due to

$$\begin{aligned} f(0, \lambda) &= \left(\frac{\lambda + \overline{c}_T}{\overline{c}_T} \right), \\ f(x_G^*, \lambda) &= - \left(\frac{\overline{c}_G \overline{w}_G}{\overline{c}_T} \right) (\hat{y} x_G^*) + \left(\frac{\lambda + \overline{c}_T}{\overline{c}_T} \right). \end{aligned}$$

2. The graph of $y = f(x, \lambda)$ in the xy -plane is concave up, due to the leading coefficient $(\overline{c}_G \overline{w}_G / \overline{c}_T)$.
3. The same graph also has its vertex point (\hat{x}_0, f_{\min}) , where

$$\hat{x}_0 := \frac{\hat{y} + x_G^*}{2}, \quad f_{\min} := f(\hat{x}_0, \lambda) = f(0, \lambda) - \left(\frac{\overline{c}_G \overline{w}_G}{\overline{c}_T} \right) \hat{x}_0^2.$$

Thus, $f(x, \lambda)$ decreases with negative $\frac{\partial f}{\partial x}$ for $x < \hat{x}_0$ and increases with positive $\frac{\partial f}{\partial x}$ for $x > \hat{x}_0$.

4. We have $2(\hat{x}_0 - x_G^*) = \hat{y} - x_G^*$, hence $\operatorname{sgn}(\hat{x}_0 - x_G^*) = \operatorname{sgn}(\hat{y} - x_G^*)$. Moreover, $\hat{x}_0 \leq x_G^*$ if $\hat{y} \leq x_G^*$.

5. Finally, the quadratic formula gives the following roots of $f(\cdot, \lambda) - 1$:

$$\begin{aligned}\hat{x}_1 &:= \hat{x}_0 - \sqrt{\hat{x}_0^2 - \frac{\bar{c}_T}{\bar{c}_G w_G} [f(0, \lambda) - 1]}, \\ \hat{x}_2 &:= \hat{x}_0 + \sqrt{\hat{x}_0^2 - \frac{\bar{c}_T}{\bar{c}_G w_G} [f(0, \lambda) - 1]}.\end{aligned}$$

Note that $\hat{x}_1 \leq \hat{x}_2$.

For a simpler analytical approach, we may consider the following set

$$\begin{aligned}\mathcal{I}_0 &:= \{x \mid 0 < x \leq x_G^* \text{ and } f(x, \lambda) > 1\}, \\ \implies \mathcal{I} &= \mathcal{I}_0 \cap \left\{ x \mid \mu \leq \mathcal{H}_G^* \text{ or } f(x, \lambda) \leq \frac{\mu}{\mu - \mathcal{H}_G^*} \right\}.\end{aligned}$$

Then Theorem 3 implies that $E^* \in \mathcal{I}_0$. That is, \mathcal{I}_0 provides regions to locate E^* , while \mathcal{I} provides additional restriction.

To determine the possible sets that \mathcal{I}_0 takes, we appeal to the monotone and concave properties of $f(\cdot, \lambda)$, particularly that $f(x, \lambda)$ decreases for $x < \hat{x}_0$ and increases for $x > \hat{x}_0$. Consider partitioning the parameter space into the following cases.

- Case 1: $f(0, \lambda) \leq 1$.

If $\hat{x}_0 > x_G^*$, then $f(x, \lambda)$ decreases with x over $(0, x_G^*]$. Otherwise, the image of $(0, x_G^*]$ under $f(\cdot, \lambda)$ is $[f_{\min}, f(0, \lambda)) \subset (-\infty, 1)$. Therefore, \mathcal{I}_0 is empty.

- Case 2: $f(x_G^*, \lambda) \leq 1 < f(0, \lambda)$.

Restricting $f(x, \lambda)$ for $0 < x < x_G^*$ and following the same cases for \hat{x}_0 , we see that $f(x, \lambda) = 1$ uniquely at $x = \hat{x}_1$. Moreover, $\mathcal{I}_0 = (0, \hat{x}_1)$, with $f(x, \lambda) > 1$ for $0 < x < \hat{x}_1$, and $f(x, \lambda) < 1$ for $\hat{x}_1 < x \leq x_G^*$.

- Case 3: $f(x_G^*, \lambda) > 1$, and either $\hat{y} \geq x_G^*$ or $f_{\min} > 1$.

Note in this case that $f(0, \lambda) > f(x_G^*, \lambda) > 1$. If $\hat{y} \geq x_G^*$ (equivalently, $\hat{x}_0 \geq x_G^*$), then as x increases from zero to x_G^* , the value of f decreases from $f(0, \lambda)$ to $f(x_G^*, \lambda) > 1$. Otherwise, with $f_{\min} > 1$, the image of $(0, x_G^*]$ under $f(\cdot, \lambda)$ is $[f_{\min}, f(0, \lambda)) \supset (1, \infty)$. Therefore, $\mathcal{I}_0 = (0, x_G^*]$.

- Case 4: $f(x_G^*, \lambda) > 1$, $\hat{y} < x_G^*$ (equivalently $\hat{x}_0 < x_G^*$), and $f_{\min} \leq 1$.

Here, both $f(0, \lambda)$ and $f(x_G^*, \lambda)$ are above one, but $f_{\min} \leq 1$. Thus, the roots \hat{x}_1 and \hat{x}_2 of $f(\cdot, \lambda)$ exist, with $\hat{x}_1 \leq \hat{x}_0 \leq \hat{x}_2$. Since $f(x, \lambda)$ decreases for $x < \hat{x}_0$ and increases for $x > \hat{x}_0$, we conclude that $\mathcal{I}_0 = (0, \hat{x}_1) \cup (\hat{x}_2, x_G^*]$.

Table S1

Different cases for the set \mathcal{I}_0 . All cases assume that $\lambda > -\overline{c_T}$, which is necessary for E^* to exist (Theorem 2).

| Case | Conditions | Set \mathcal{I}_0 |
|------|--|--|
| 1 | $-\overline{c_T} < \lambda \leq 0$ | Empty |
| 2 | $0 < \lambda \leq \Lambda_1$ | $(0, \hat{x}_1)$ |
| 3 | $\lambda > \Lambda_1$, and either $\hat{x}_0 \geq x_G^*$ or $\lambda > \Lambda_2$ | $(0, x_G^*]$ |
| 4 | $\hat{x}_0 < x_G^*$ and $\Lambda_1 < \lambda \leq \Lambda_2$ | $(0, \hat{x}_1) \cup (\hat{x}_2, x_G^*]$ |

We may express the conditions of the four cases in λ by writing

$$\begin{aligned} f(0, \lambda) - 1 &= \lambda(\overline{c_T})^{-1}, \\ f(x_G^*, \lambda) - 1 &= \frac{\lambda - \Lambda_1}{\overline{c_T}}, \\ f_{\min} - 1 &= \frac{\lambda - \Lambda_2}{\overline{c_T}}, \end{aligned}$$

where

$$\begin{aligned} \Lambda_1 &:= (\overline{c_G} \overline{w_G})(2\hat{x}_0 - x_G^*)x_G^* = (\overline{c_G} \overline{w_G})\hat{y}x_G^*, \\ \Lambda_2 &:= (\overline{c_G} \overline{w_G})\hat{x}_0^2. \end{aligned}$$

These yield the following sign equations

$$\begin{aligned} \operatorname{sgn}[f(0, \lambda) - 1] &= \operatorname{sgn} \lambda, \\ \operatorname{sgn}[f(x_G^*, \lambda) - 1] &= \operatorname{sgn}(\lambda - \Lambda_1), \\ \operatorname{sgn}(f_{\min} - 1) &= \operatorname{sgn}(\lambda - \Lambda_2), \end{aligned}$$

in addition to $\operatorname{sgn}(\hat{x}_0 - x_G^*) = \operatorname{sgn}(\hat{y} - x_G^*)$. Table S1 summarizes our analysis on the different intervals (or union of intervals) that \mathcal{I}_0 takes.

We now investigate the equation

$$\mathcal{H}(\cdot, \overline{K_T}) = \mu \mathcal{H}_0(\cdot, \lambda) \text{ on } \mathcal{I}_0 \tag{39}$$

from Eq. (28), where the root(s) determine the viral load size(s) x^* at E^* . We have

$$\frac{\partial \mathcal{H}}{\partial x} = \frac{m \overline{K_T}^m \cdot x^{m-1}}{(x^m + \overline{K_T}^m)^2} > 0 \quad \text{for } x > 0, \tag{40}$$

so $\mathcal{H}(\cdot, \overline{K_T})$ increases over $(0, x_G^*]$ and particularly over \mathcal{I}_0 . On the other hand, we can determine the monotone properties of $\mathcal{H}_0(\cdot, \lambda)$ by applying Eqs. (25) and (26), assuming that $f > 0$. Now,

$$\begin{aligned}\frac{\partial f}{\partial x} &= \left(\frac{\overline{c_G} \overline{w_G}}{\overline{c_T}} \right) [2x - (\hat{y} + x_G^*)] \\ &= 2 \left(\frac{\overline{c_G} \overline{w_G}}{\overline{c_T}} \right) (x - \hat{x}_0).\end{aligned}\tag{41}$$

Then

$$\begin{aligned}\frac{\partial \mathcal{H}_0}{\partial x} &= \frac{\partial}{\partial x} \left(1 - \frac{1}{f} \right) = \frac{1}{f^2} \frac{\partial f}{\partial x} \\ &= \frac{2}{[f(x, \lambda)]^2} \left(\frac{\overline{c_G} \overline{w_G}}{\overline{c_T}} \right) (x - \hat{x}_0).\end{aligned}\tag{42}$$

For concavity, we may compute the following second partial derivative:

$$\begin{aligned}\frac{\partial^2 \mathcal{H}_0}{\partial x^2} &= \frac{2}{[f(x, \lambda)]^3} \left(\frac{\overline{c_G} \overline{w_G}}{\overline{c_T}} \right) \left[2(\hat{x}_0 - x) \frac{\partial f}{\partial x} + f \right] \\ &= \frac{2}{[f(x, \lambda)]^3} \left(\frac{\overline{c_G} \overline{w_G}}{\overline{c_T}} \right) \left[f(x, \lambda) - 4 \left(\frac{\overline{c_G} \overline{w_G}}{\overline{c_T}} \right) (x - \hat{x}_0)^2 \right] \\ &= \frac{8}{[f(x, \lambda)]^3} \left(\frac{\overline{c_G} \overline{w_G}}{\overline{c_T}} \right)^2 \left[\frac{1}{4} \left(\frac{\overline{c_T}}{\overline{c_G} \overline{w_G}} \right) f(x, \lambda) - (x - \hat{x}_0)^2 \right].\end{aligned}\tag{43}$$

Since $f(\cdot, \lambda) > 1 > 0$ on \mathcal{I}_0 , Eqs. (41)-(43) yield the following sign equations for all $x \in \mathcal{I}_0$:

$$\operatorname{sgn} \frac{\partial \mathcal{H}_0}{\partial x} = \operatorname{sgn}(x - \hat{x}_0) = \operatorname{sgn} \frac{\partial f}{\partial x},\tag{44}$$

$$\operatorname{sgn} \frac{\partial^2 \mathcal{H}_0}{\partial x^2} = \operatorname{sgn} \left[\frac{1}{4} \left(\frac{\overline{c_T}}{\overline{c_G} \overline{w_G}} \right) f(x, \lambda) - (x - \hat{x}_0)^2 \right].\tag{45}$$

In particular, both $\mathcal{H}_0(\cdot, \lambda)$ and $f(\cdot, \lambda)$ share the same monotone properties over \mathcal{I}_0 . We also note that

$$\operatorname{sgn} \mathcal{H}_0(0, \lambda) = \operatorname{sgn}[f(0, \lambda) - 1]$$

Armed with these observations, we revisit Cases 2-4 in Table S1. We skip Case 1 because \mathcal{I}_0 is empty and thus E^* does not exist. For Cases 2-4, $f(0, \lambda) > 1$ and $\mathcal{H}_0(0, \lambda) > 0$. Recalling $\mu = \overline{\delta_T}/\overline{r_T}$, the signs of \mathcal{H}_0 , $\mu \mathcal{H}_0$ and their partial derivatives are equal. Eq. (28), we also have

- Under Case 2, we have $\mathcal{I}_0 = (0, \hat{x}_1) \subseteq (0, \hat{x}_0)$. Hence by eq. (42), $\mathcal{H}_0(\cdot, \lambda)$ decreases over \mathcal{I}_0 . Considering

eq. (40) and that

$$\mu \mathcal{H}_0(\hat{x}_1, \lambda) = 0 < \mu \mathcal{H}_0(0, \lambda),$$

Eq. (39) admits exactly one solution x^* .

- Under Case 3, we now have $\mathcal{I}_0 = (0, x_G^*]$ so that $\mathcal{H}_0(x, \lambda) > 0$ for $0 < x \leq x_G^*$. We proceed with the following subcases:

- Subcase 3a. If $\hat{x}_0 \geq x_G^*$, then according to Eq. (44) we have $\frac{\partial \mathcal{H}_0}{\partial x} < 0$ and $\mathcal{H}_0(\cdot, \lambda)$ decreases over \mathcal{I}_0 . Furthermore, eq. (39) admits a solution if and only if

$$\mu \mathcal{H}_0(x_G^*, \lambda) \leq \mathcal{H}(x_G^*, \overline{K_T}) = \mathcal{H}_G^*.$$

This solution is unique due to the decreasing property of $\mathcal{H}_0(\cdot, \lambda)$.

- Subcase 3b. If $0 < \hat{x} < x_G^*$, then $\mathcal{H}_0(\cdot, \lambda)$ decreases over $(0, \hat{x}_0)$ and increases over (\hat{x}_0, x_G^*) . Similar to the Subcase 3a, we conclude that Eq. (39) *restricted to* $(0, \hat{x}_0)$ has a solution (which is unique) if and only if

$$\mu \mathcal{H}_0(\hat{x}, \lambda) \leq \mathcal{H}(\hat{x}, \overline{K_T}).$$

Over $(\hat{x}_0, x_G^*]$, the behavior of Eq. (39) may be intricate due to the changing convexities of both functions $\mathcal{H}(\cdot, \overline{K_T})$ and $\mu \mathcal{H}_0(\cdot, \lambda)$. Future work may need to determine possible numbers of roots of Eq. eq. (39) over $(\hat{x}_0, x_G^*]$.

- Finally, we have $\mathcal{I}_0 = (0, \hat{x}_1) \cup (\hat{x}_2, x_G^*]$ (disjoint union of intervals) in Case 4. Similar to Case 1, we find that Eq. (39) attains a unique solution over $(0, \hat{x}_1)$. Similar to Case 3b, we might expect the same kind of intricate behavior of Eq. (39) over $(\hat{x}_2, x_G^*]$ depending on μ and the concave properties of \mathcal{H} and \mathcal{H}_0 .

We are ready to consolidate our analysis on the existence of virus-positive equilibria. Anticipating the possibility of more than one virus-positive equilibrium points, we may write $\mathcal{H} - \mu \mathcal{H}_0$ as a rational function in x , where both the numerator and the denominator are polynomials in x of degree $m+2$. Hence, we deduce that the equation $\mathcal{H}(\cdot, \overline{K_T}) = \mu \mathcal{H}_0(\cdot, \lambda)$ admits at most $m+2$ distinct roots in \mathcal{I}_0 . We will denote these roots as $x_1^*, x_2^*, \dots, x_\ell^*$, where $\ell \leq m+2$ and $x_j < x_k$ for $j < k$ (provided both x_j and x_k exist). These roots correspond to the existence of the virus-positive

equilibrium points

$$E_k^* = (x_k^*, f(x_k^*, \lambda), x_k^*, \overline{w_M}x_k^*, \overline{w_G}x_k^*(x_G^* - x_k^*)), \quad k = 1, 2, \dots, \ell.$$

The number ℓ determines how many virus-positive equilibrium points exist, so that $\ell = 0$ means that the only equilibrium point is virus-free (i.e., E_0). In the simplest case where $m = 2$, we can expect up to four virus-positive equilibrium points ($\ell \leq 4$).

We consolidate our preceding analysis, especially Table S1 and Theorems 2 and 3, into the following summary.

Theorem 4. *Dimensionless Model 6, Eqs. (16)-(20), admits virus-positive equilibrium points only if $\lambda > 0$. Under this condition, we have the following cases:*

- (a) *If $0 < \lambda \leq \Lambda_1$, then $\ell = 1$ and E_1^* is the unique virus-positive equilibrium point. Furthermore, $x_1^* \in (0, \hat{x}_1)$.*
- (b) *If $\lambda > \Lambda_1$ and $\hat{x}_0 \geq x_G^*$, then $\ell = 1$ and the virus-positive equilibrium point E_1^* exists with $x_1^* \in (0, x_G^*]$.*
- (c) *Suppose that $\lambda > \Lambda_1$ but $\hat{x}_0 < x_G^*$, and $\lambda > \Lambda_2$. Then E_k^* exists with $x_k^* \in (\hat{x}_0, x_G^*]$ for $k = 2, \dots, \ell$. Moreover:*
 - *If $\mu \mathcal{H}_0(\hat{x}, \lambda) \leq \mathcal{H}(\hat{x}, \overline{K_T})$, then $x_1^* \in (0, \hat{x}_0)$ and $\ell \geq 1$.*
 - *Otherwise, $x_1^* \in (\hat{x}_0, x_G^*]$ and we can only conclude that $\ell \geq 0$. Here, the value of ℓ may depend on the concavity of \mathcal{H} and $\mu \mathcal{H}_0$.*
- (d) *Suppose that $\hat{x}_0 < x_G^*$ and $\Lambda_1 < \lambda \leq \Lambda_2$. Then $\ell \geq 1$ and E_1^* exists with $x_1^* \in (0, \hat{x}_1)$. Moreover, E_k^* exists with $x_k^* \in (\hat{x}_2, x_G^*]$ for $k = 2, \dots, \ell$.*

Remark. Further analysis, either through numerical exploration or advanced mathematical tools, is needed in the following cases:

- $\lambda > \max(\Lambda_1, \Lambda_2)$ and $\hat{x}_0 < x_G^*$.
- $\hat{x}_0 < x_G^*$ and $\Lambda_1 < \lambda \leq \Lambda_2$, only for the equilibrium points E_2^*, \dots, E_ℓ^* .

B. Math Modelling

B.1. Model 2

$$\frac{dV}{dt} = pV \left(1 - \frac{V}{K_V}\right) - c_t VT - \varepsilon MV - \eta GV - cV, \quad (46)$$

$$\frac{dT}{dt} = \delta_t T(0) + rT \left(\frac{V^m}{V^m + k_t^m}\right) - \delta_t T, \quad (47)$$

$$\frac{dM}{dt} = \alpha V(t - \tau_1) - (\gamma + \beta)M, \quad (48)$$

$$\frac{dG}{dt} = \gamma M + \lambda V(t - \tau_2) - \rho G. \quad (49)$$

B.2. Model 4

$$\frac{dV}{dt} = pV \left(1 - \frac{V}{K_V}\right) - c_t VT - \varepsilon MV - \eta GV - cV, \quad (50)$$

$$\frac{dT}{dt} = \delta_t T(0) + rT \left(\frac{V^m}{V^m + k_t^m}\right) - \delta_t T, \quad (51)$$

$$\frac{dB}{dt} = r_b \left(\frac{1}{1 + l_v V}\right) \left(\frac{1}{1 + l_t T}\right) (1 - B), \quad (52)$$

$$\frac{dM}{dt} = r_m B - (q + \delta_m)M, \quad (53)$$

$$\frac{dG}{dt} = qM + r_g B - \delta_g G. \quad (54)$$

B.3. Model 5

$$\frac{dV}{dt} = pV \left(1 - \frac{V}{K_V}\right) - c_t VT - \varepsilon MV - \eta GV - cV, \quad (55)$$

$$\frac{dT}{dt} = \delta_t T(0) + rT \left(\frac{V^m}{V^m + k_t^m}\right) - \delta_t T, \quad (56)$$

$$\frac{dB}{dt} = \frac{\delta_v V - B}{\tau_b}, \quad (57)$$

$$\frac{dM}{dt} = r_m B - (q + \delta_m)M, \quad (58)$$

$$\frac{dG}{dt} = q \left(\frac{M^n}{M^n + k_q^n}\right) + r_g B - \delta_g G. \quad (59)$$

C. AIC scores for each severe patients

Table S2

AIC scores for severe patients

| Patient | AIC Model 1 | AIC Model 2 | AIC Model 3 | AIC Model 4 | AIC Model 5 | AIC Model 6 |
|---------|-------------|-------------|-------------|-------------|-------------|-------------|
| 2 | 7.32 | -5.74 | -13.24 | -42.57 | -57.92 | -63.02 |
| 3 | 35.86 | 12.52 | 23.75 | -12.63 | -36.84 | -15.46 |
| 5 | 21.08 | -6.24 | 1.32 | -32.61 | -11.72 | -28.25 |
| 12 | 14.63 | -1.02 | -32.70 | -30.84 | -20.93 | -18.76 |
| 15 | 27.37 | -4.27 | -14.59 | -19.52 | -5.96 | -19.13 |
| 20 | 42.60 | 4.85 | 4.85 | -31.08 | -29.41 | -9.26 |
| 34 | 16.93 | 7.29 | -1.19 | -28.85 | -25.74 | -34.49 |
| Media | 23.68 | 1.05 | -4.54 | -28.30 | -26.93 | -26.91 |

D. AIC scores for each non-severe patients

Table S3

AIC scores for each non-severe patients

| Patient | AIC Model 1 | AIC Model 2 | AIC Model 3 | AIC Model 4 | AIC Model 5 | AIC Model 6 |
|---------|-------------|-------------|-------------|-------------|-------------|-------------|
| 1 | 32.57 | 25.76 | 6.23 | 4.84 | -36.1 | -13.65 |
| 4 | 4.56 | 13.57 | -20.36 | -59.27 | -24.82 | -166.21 |
| 7 | 57.34 | 34.08 | 5.25 | -8.29 | -3.73 | -13.32 |
| 8 | 25.78 | 11.41 | -16.39 | -2.04 | -14.42 | -24.88 |
| 9 | 9.47 | -2.69 | -18.87 | 4.06 | -25.38 | -29.18 |
| 13 | -5.12 | 7.63 | -48.31 | -7.49 | -16.11 | -61.75 |
| 14 | 12.45 | 19.54 | 3.48 | -8.16 | -17.93 | -36.27 |
| 16 | 41.63 | 23.97 | 4.72 | -2.93 | 11.03 | -9.49 |
| 17 | 6.28 | 25.06 | -1.38 | -17.26 | -6.49 | -19.32 |
| 18 | -3.93 | 17.42 | -19.65 | -11.42 | -28.53 | -25.86 |
| 19 | 5.84 | 19.70 | -3.27 | -2.98 | -26.77 | -14.09 |
| 21 | 34.72 | 2.86 | -25.93 | -36.07 | -21.53 | -48.30 |
| 22 | 23.67 | -4.84 | -2.21 | -12.30 | -9.64 | -7.38 |
| 24 | 11.63 | 10.65 | -23.74 | -2.04 | -35.23 | -27.10 |
| 25 | -7.32 | 38.32 | -43.91 | -55.72 | -85.41 | -173.52 |
| 26 | 17.48 | 3.05 | -16.01 | -28.04 | -21.63 | -37.16 |
| 27 | 9.37 | 23.94 | -2.72 | 2.63 | -37.50 | -18.56 |
| 29 | 17.82 | -7.13 | 12.54 | -28.42 | -26.94 | -30.22 |
| 31 | 16.21 | 4.21 | 3.90 | -12.63 | -33.71 | -45.27 |
| 35 | 8.84 | -12.74 | 11.34 | -27.75 | -52.02 | -63.34 |
| 36 | 19.36 | -18.95 | 2.45 | -9.03 | -5.94 | -12.89 |
| 37 | 26.21 | 11.62 | -47.25 | -2.49 | -16.83 | 6.81 |
| 38 | 21.45 | 4.29 | -15.68 | -24.23 | -26.56 | -30.18 |
| 39 | 12.87 | -2.16 | -14.63 | -9.62 | -8.34 | -24.02 |
| 40 | 35.97 | -3.59 | 2.03 | -2.73 | 3.65 | -7.93 |
| 42 | 23.92 | -1.08 | 4.78 | -8.38 | -36.7 | -6.71 |
| 53 | 31.37 | -8.60 | -2.47 | -23.52 | -21.26 | -24.92 |
| 57 | 48.93 | -2.57 | 11.19 | -2.96 | -7.40 | -9.70 |
| 59 | 27.80 | 4.89 | 1.53 | -13.06 | -2.87 | -19.18 |
| 61 | 15.04 | 3.86 | -23.64 | -5.14 | -27.81 | -31.70 |
| 63 | 48.52 | -4.43 | -9.05 | 2.85 | -42.43 | -20.56 |
| 64 | 4.63 | -10.86 | -14.32 | -20.45 | -8.92 | -17.33 |
| Media | 19.85 | 7.06 | -9.38 | -13.43 | -22.32 | -33.65 |

E. Estimated parameters of Model 6 for each severe patients

Table S4

Estimated parameters for each severe patients

| Patients | c_M | c_G | τ_b | r_M | q | r_G | K_g | r_q | r_B |
|----------|----------|----------|----------|----------|----------|----------|----------|----------|----------|
| 2 | 1.24E-04 | 1.20E-04 | 2.95E+00 | 5.00E-06 | 1.00E-01 | 7.00E-06 | 2.35E+01 | 1.05E-01 | 2.33E-01 |
| 3 | 6.06E-03 | 2.93E-01 | 1.96E+01 | 1.92E-04 | 5.27E-02 | 4.77E-04 | 9.19E+00 | 7.76E+00 | 2.34E-01 |
| 5 | 2.13E-03 | 1.77E-01 | 3.23E+01 | 1.00E-06 | 7.88E-04 | 1.00E-06 | 2.13E+02 | 1.71E-01 | 1.42E-01 |
| 12 | 1.53E-03 | 1.82E-02 | 4.72E+00 | 6.64E-07 | 9.97E-02 | 1.00E-09 | 3.68E+02 | 1.76E-01 | 1.93E-01 |
| 15 | 3.35E-03 | 2.78E-02 | 3.99E+01 | 4.00E-06 | 1.35E-03 | 1.00E-09 | 3.88E+02 | 6.88E-02 | 2.17E-01 |
| 20 | 7.81E-03 | 2.40E-02 | 3.98E+01 | 2.00E-06 | 9.79E-04 | 1.00E-09 | 3.90E+02 | 1.60E-01 | 2.36E-01 |
| 34 | 8.98E-03 | 2.81E-01 | 1.50E+00 | 3.37E-04 | 7.32E-02 | 8.07E-03 | 3.74E+02 | 2.31E+01 | 1.34E-01 |

F. Estimated parameters of Model 6 for each non-severe patients

Table S5

Estimated parameters for each non-severe patients

| Patients | c_M | c_G | τ_b | r_M | q | r_G | K_g | r_q | r_B |
|----------|----------|----------|----------|----------|----------|----------|----------|----------|----------|
| 1 | 6.04E-03 | 4.08E-02 | 6.48E+00 | 1.25E-03 | 3.34E-03 | 3.03E-04 | 3.66E+02 | 9.19E-03 | 1.05E-01 |
| 4 | 9.39E-03 | 2.71E-04 | 2.56E+00 | 1.00E-09 | 8.57E-02 | 8.79E-07 | 1.02E+02 | 1.96E-02 | 1.19E-01 |
| 7 | 7.43E-03 | 2.09E-03 | 1.09E+01 | 4.75E-08 | 1.20E-04 | 4.07E-07 | 8.20E+01 | 1.04E-02 | 2.90E-01 |
| 8 | 5.11E-03 | 2.45E-01 | 3.97E+01 | 9.79E-09 | 4.01E-02 | 6.53E-07 | 9.39E+01 | 1.37E+00 | 1.10E-01 |
| 9 | 6.68E-03 | 1.47E-01 | 3.15E+01 | 2.86E-08 | 1.11E-03 | 3.00E-06 | 1.75E+02 | 2.74E-01 | 1.53E-01 |
| 13 | 9.46E-03 | 1.77E-02 | 6.68E+00 | 6.78E-07 | 4.62E-02 | 1.00E-09 | 3.82E+02 | 6.13E-01 | 1.55E-01 |
| 14 | 2.85E-03 | 7.11E-02 | 1.52E+01 | 1.00E-06 | 1.70E-03 | 1.00E-09 | 3.32E+02 | 1.55E-01 | 2.02E-01 |
| 16 | 4.92E-04 | 8.09E-03 | 3.97E+01 | 5.00E-06 | 2.78E-03 | 1.00E-09 | 3.96E+02 | 1.14E-01 | 2.19E-01 |
| 17 | 2.63E-04 | 1.45E-02 | 6.34E+00 | 7.25E-07 | 7.06E-02 | 1.00E-09 | 2.51E+02 | 5.64E-01 | 1.60E-01 |
| 18 | 4.30E-03 | 8.19E-02 | 3.97E+01 | 8.08E-07 | 4.04E-03 | 1.00E-09 | 3.80E+02 | 9.63E-02 | 9.18E-01 |
| 19 | 3.43E-04 | 2.16E-01 | 3.98E+01 | 8.57E-07 | 9.20E-04 | 1.00E-09 | 3.87E+02 | 3.91E-02 | 5.83E-01 |
| 21 | 7.83E-04 | 2.90E-01 | 2.18E+01 | 1.00E-06 | 3.86E-03 | 1.00E-09 | 3.95E+02 | 2.37E-02 | 3.15E-01 |
| 22 | 5.56E-03 | 2.87E-01 | 3.88E+01 | 6.79E-07 | 2.68E-03 | 1.00E-09 | 3.97E+02 | 1.78E-02 | 7.56E-01 |
| 24 | 6.00E-03 | 7.21E-02 | 8.25E+00 | 9.00E-07 | 5.80E-02 | 1.00E-09 | 3.29E+02 | 1.11E-01 | 1.60E-01 |
| 25 | 7.20E-03 | 2.66E-01 | 3.70E+01 | 6.32E-08 | 9.93E-02 | 1.06E-09 | 3.89E+02 | 1.34E+00 | 1.03E-01 |
| 26 | 8.18E-03 | 2.51E-01 | 3.99E+01 | 1.32E-07 | 7.82E-04 | 1.29E-09 | 2.79E+02 | 3.02E-01 | 1.02E-01 |
| 27 | 2.44E-03 | 4.75E-03 | 1.07E+01 | 4.69E-07 | 3.28E-02 | 1.05E-09 | 3.96E+02 | 7.59E-02 | 4.62E-01 |
| 29 | 3.05E-03 | 1.50E-01 | 3.49E+01 | 2.24E-09 | 4.85E-02 | 8.73E-08 | 9.60E+01 | 1.38E+00 | 1.27E-01 |
| 31 | 6.38E-03 | 2.88E-01 | 2.37E+00 | 1.63E-09 | 2.31E-02 | 2.31E-07 | 1.66E+02 | 5.10E+00 | 1.09E-01 |
| 35 | 8.11E-03 | 5.70E-04 | 2.21E+00 | 4.79E-08 | 1.15E-02 | 3.00E-06 | 3.33E+02 | 2.34E+00 | 1.16E-01 |
| 36 | 4.48E-03 | 3.00E-01 | 1.00E+00 | 1.00E-09 | 1.00E-01 | 1.00E-02 | 3.03E+02 | 2.27E+01 | 7.82E-01 |
| 37 | 1.92E-03 | 3.95E-04 | 3.16E+01 | 4.10E-05 | 6.75E-03 | 9.37E-08 | 9.19E+01 | 1.10E+00 | 1.42E-01 |
| 38 | 2.21E-03 | 1.55E-01 | 3.35E+01 | 8.76E-08 | 2.56E-02 | 3.23E-08 | 2.05E+02 | 5.64E-01 | 3.62E-01 |
| 39 | 7.75E-03 | 1.93E-01 | 3.18E+01 | 2.00E-06 | 9.60E-02 | 2.00E-06 | 1.66E+02 | 1.68E+00 | 1.15E-01 |
| 40 | 3.09E-03 | 1.56E-01 | 1.00E+00 | 2.00E-05 | 1.00E-01 | 2.60E-05 | 3.69E+02 | 1.12E+01 | 1.06E-01 |
| 42 | 4.11E-04 | 5.19E-04 | 3.99E+01 | 8.00E-06 | 2.14E-03 | 1.00E-09 | 3.99E+02 | 5.09E-01 | 1.85E-01 |
| 53 | 9.56E-03 | 1.09E-01 | 3.81E+01 | 5.77E-09 | 9.99E-02 | 1.55E-09 | 3.76E+02 | 1.75E+00 | 1.15E-01 |
| 57 | 1.00E-02 | 3.00E-01 | 1.00E+00 | 6.50E-03 | 1.00E-01 | 1.00E-02 | 1.78E+02 | 4.00E+01 | 1.00E-01 |
| 59 | 8.97E-03 | 2.04E-01 | 1.12E+00 | 1.00E-09 | 1.00E-01 | 7.93E-04 | 3.23E+02 | 3.08E+01 | 1.12E-01 |
| 61 | 7.89E-03 | 2.70E-01 | 3.04E+01 | 3.94E-08 | 5.35E-02 | 4.97E-07 | 3.39E+02 | 3.49E+00 | 1.05E-01 |
| 63 | 4.09E-03 | 5.71E-03 | 3.18E+00 | 1.00E-06 | 1.94E-03 | 6.21E-07 | 1.80E+02 | 5.04E-01 | 1.24E-01 |
| 64 | 8.80E-03 | 2.95E-01 | 4.08E+00 | 1.14E-03 | 3.14E-02 | 7.29E-04 | 4.81E+00 | 9.86E+00 | 1.48E-01 |

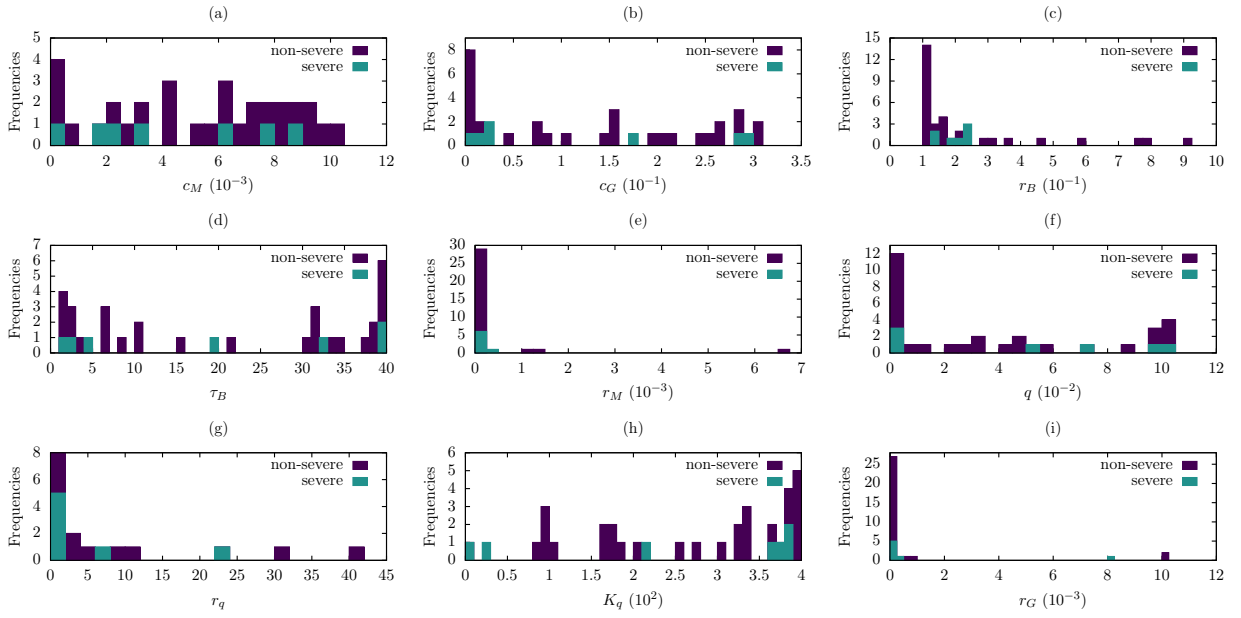


Figure S1: Parameter distributions for 7 severe patients (green) and 32 non-severe patients (purple).

G. Dynamics of Model 6 for each patient

Dynamics of viral load and immune response for each patient using the Model 6 and the parameter estimated from IgG antibody data of each patient reported in [21]. Severe D patients are presented in yellow color, severe E patients are presented in green color, and non-severe patients are presented in purple color. In each figure: (a) Viral load, (b) T cell level, (c) B cell level, (d) IgM antibody level, (e) IgG antibody level; solid line is the model output and the dots are the data.

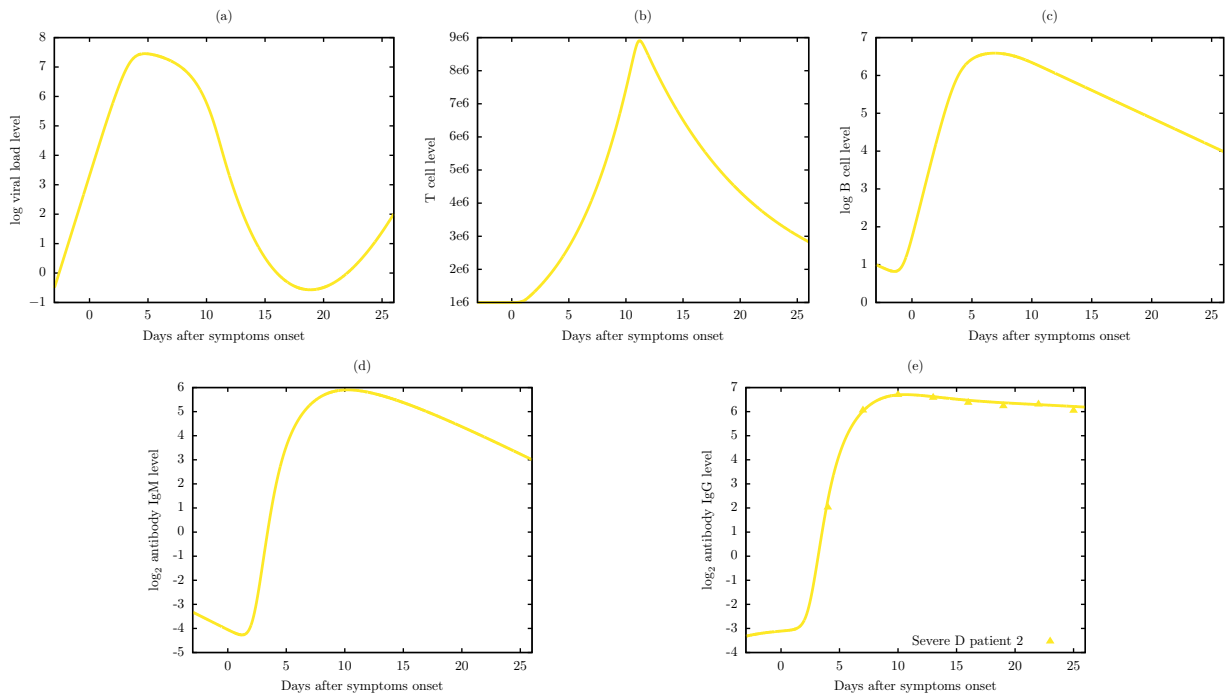


Figure S2: Viral dynamic and immune response of Model 6 for severe D patient 2.

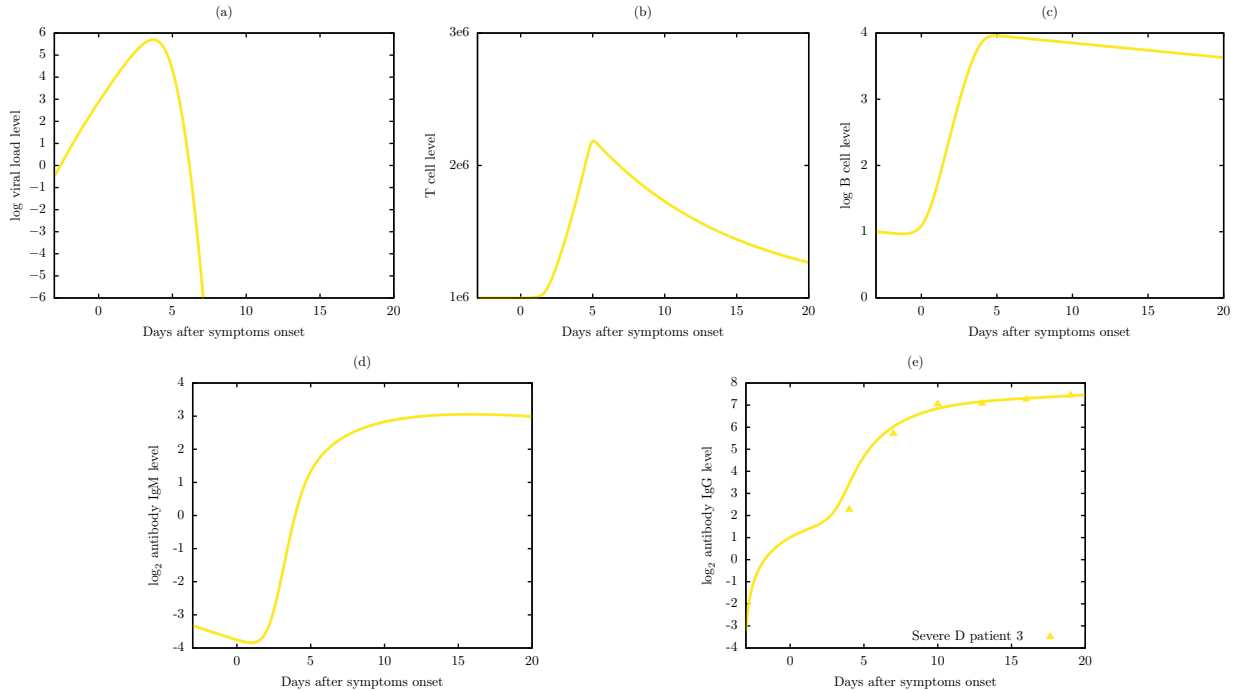


Figure S3: Viral dynamic and immune response of Model 6 for severe D patient 3.

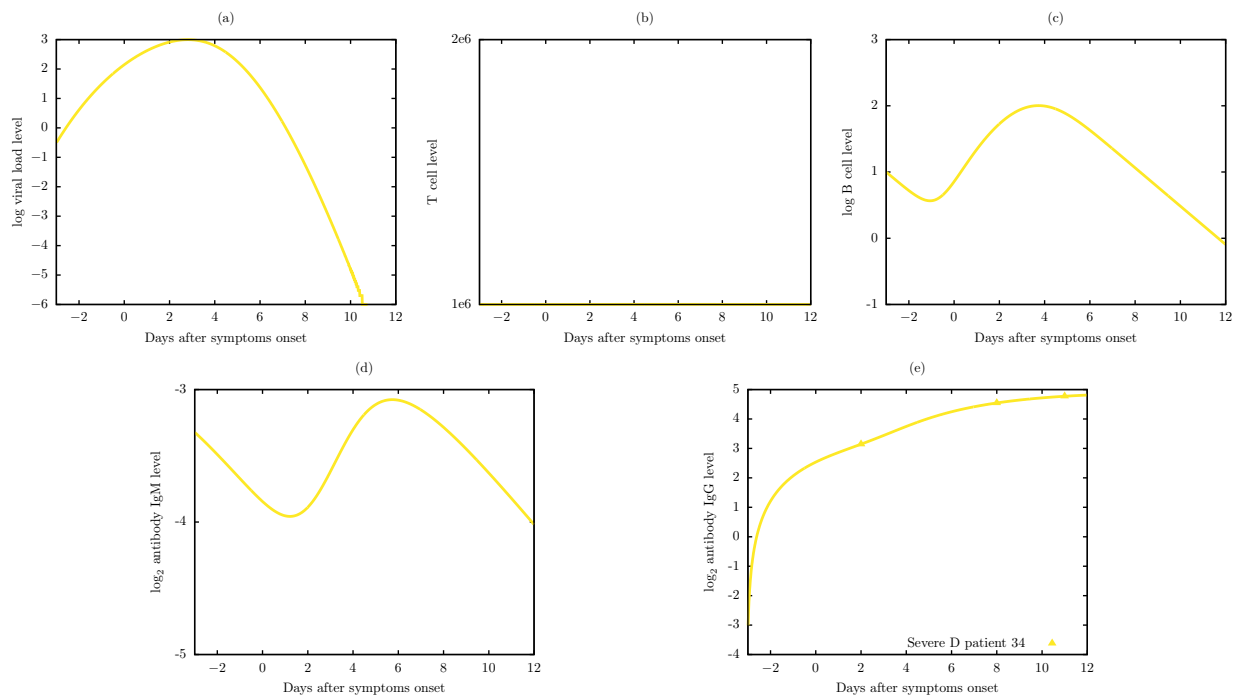


Figure S4: Viral dynamic and immune response of Model 6 for severe D patient 34.

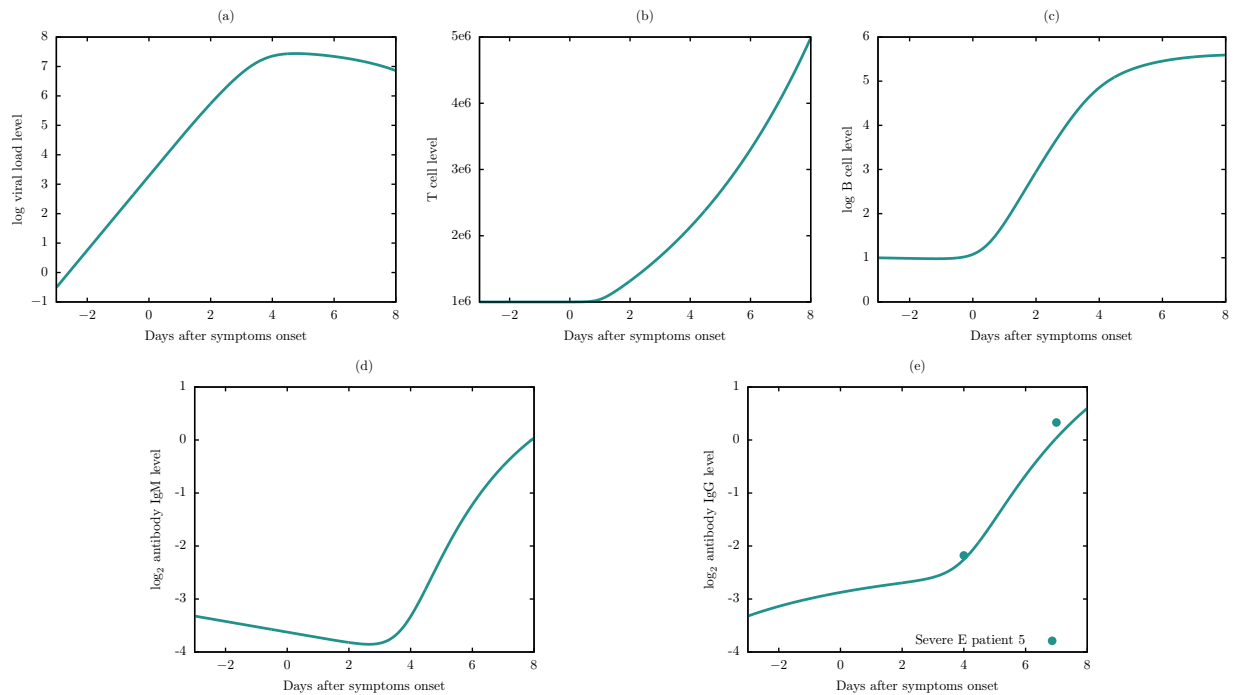


Figure S5: Viral dynamic and immune response of Model 6 for severe E patient 5.

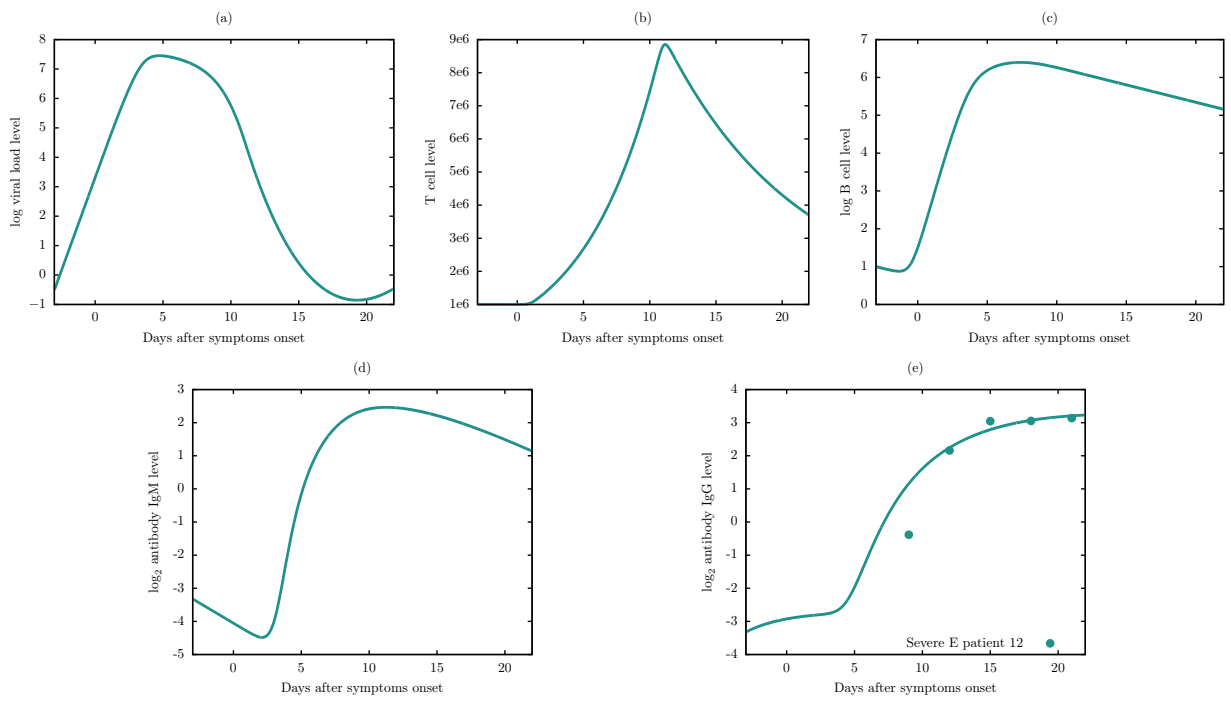


Figure S6: Viral dynamic and immune response of Model 6 for severe E patient 12.

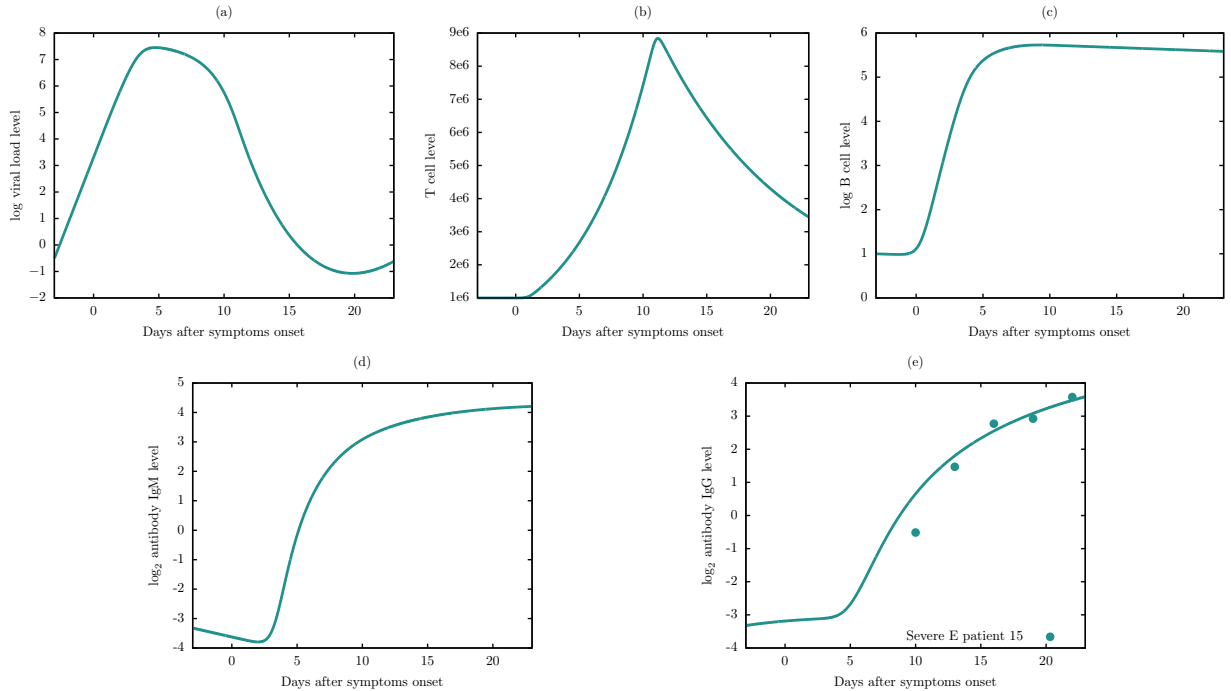


Figure S7: Viral dynamic and immune response of Model 6 for severe E patient 15.

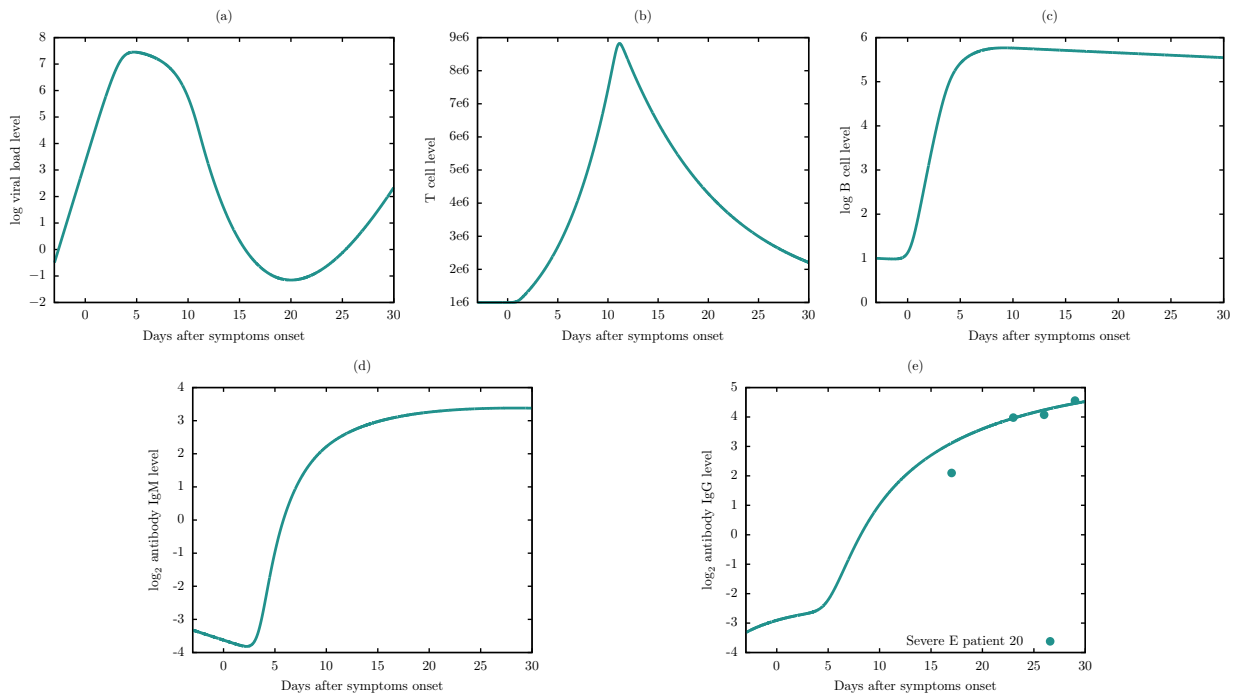


Figure S8: Viral dynamic and immune response of Model 6 for severe E patient 20.

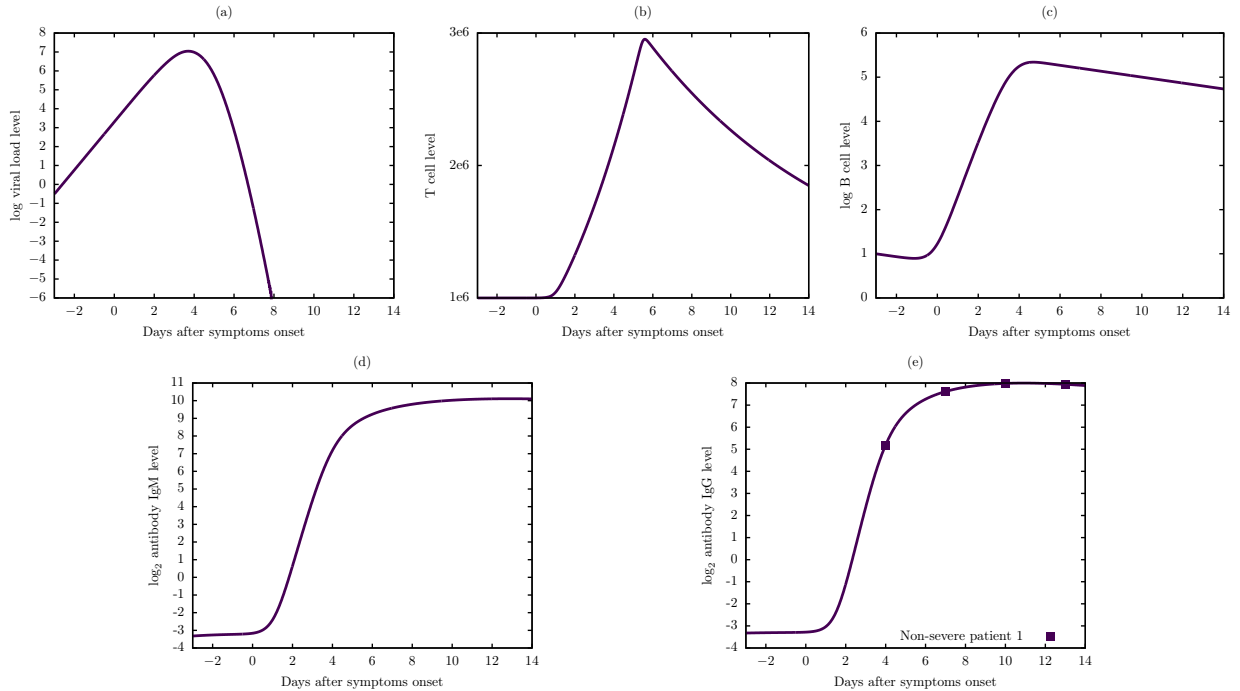


Figure S9: Viral dynamic and immune response of Model 6 for non-severe patient 1.

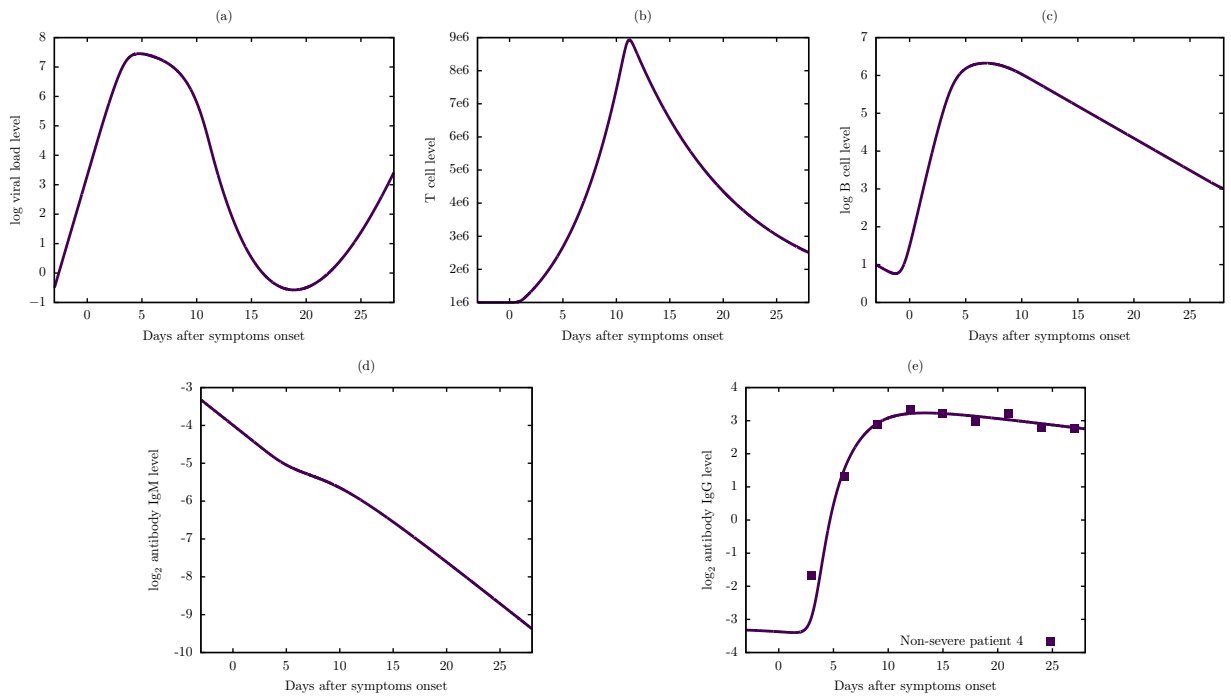


Figure S10: Viral dynamic and immune response of Model 6 for non-severe patient 4.

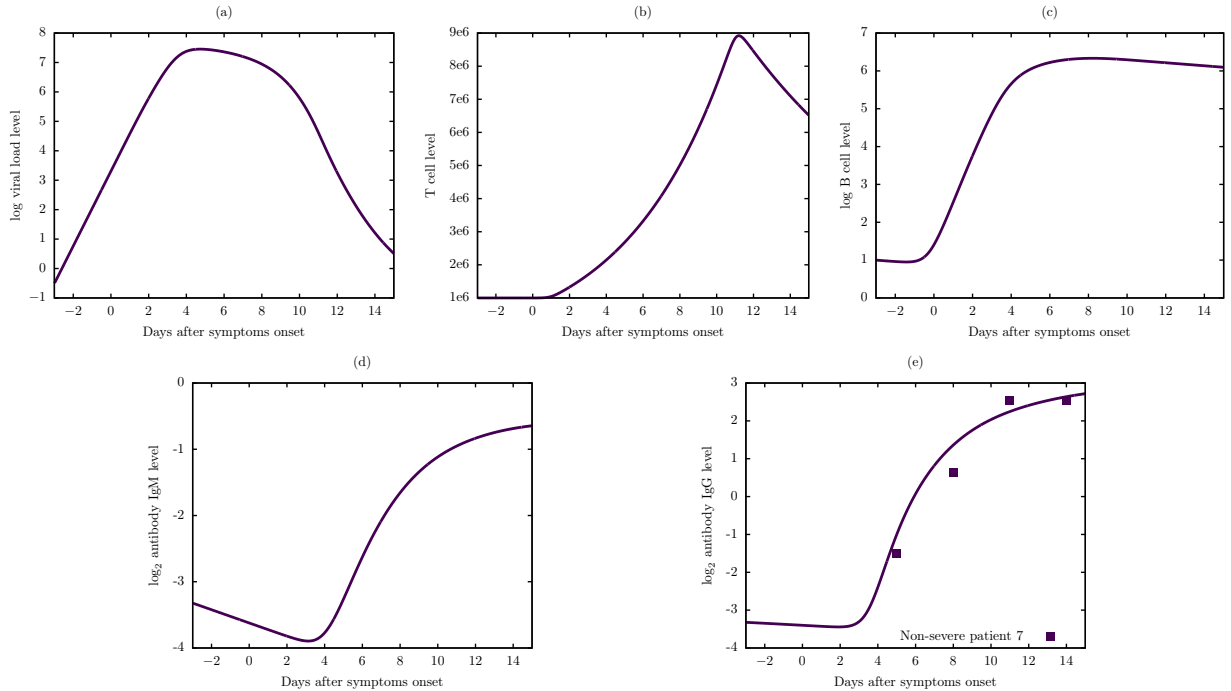


Figure S11: Viral dynamic and immune response of Model 6 for non-severe patient 7.

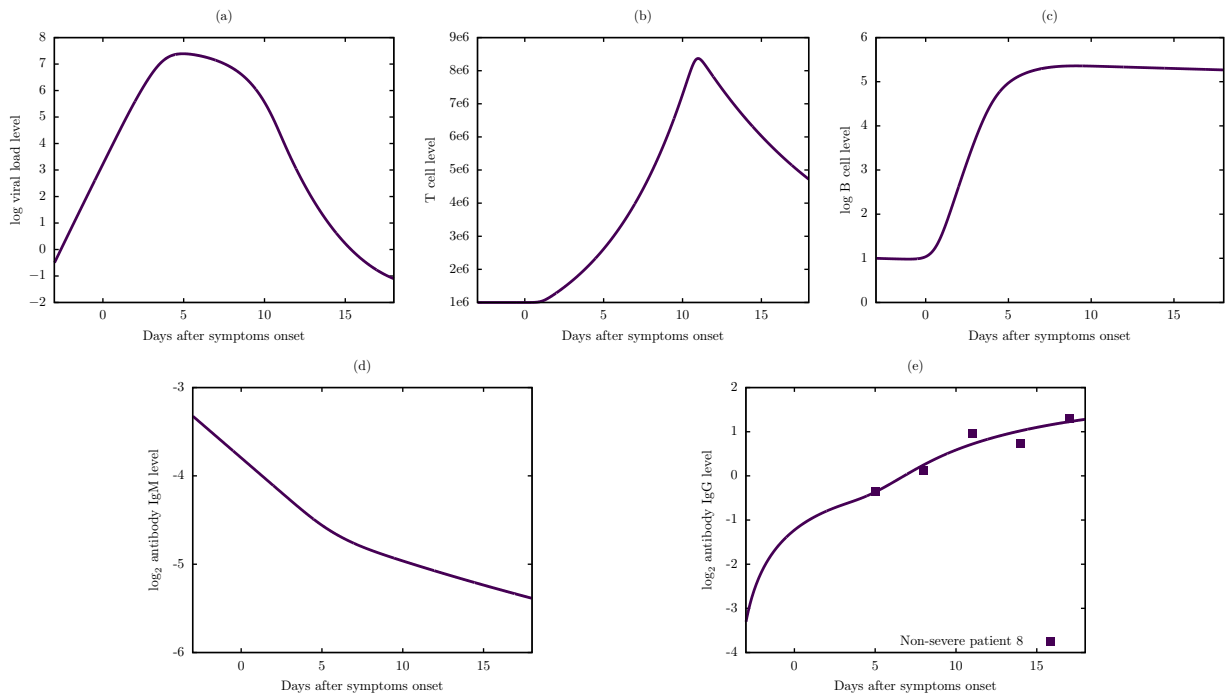


Figure S12: Viral dynamic and immune response of Model 6 for non-severe patient 8.

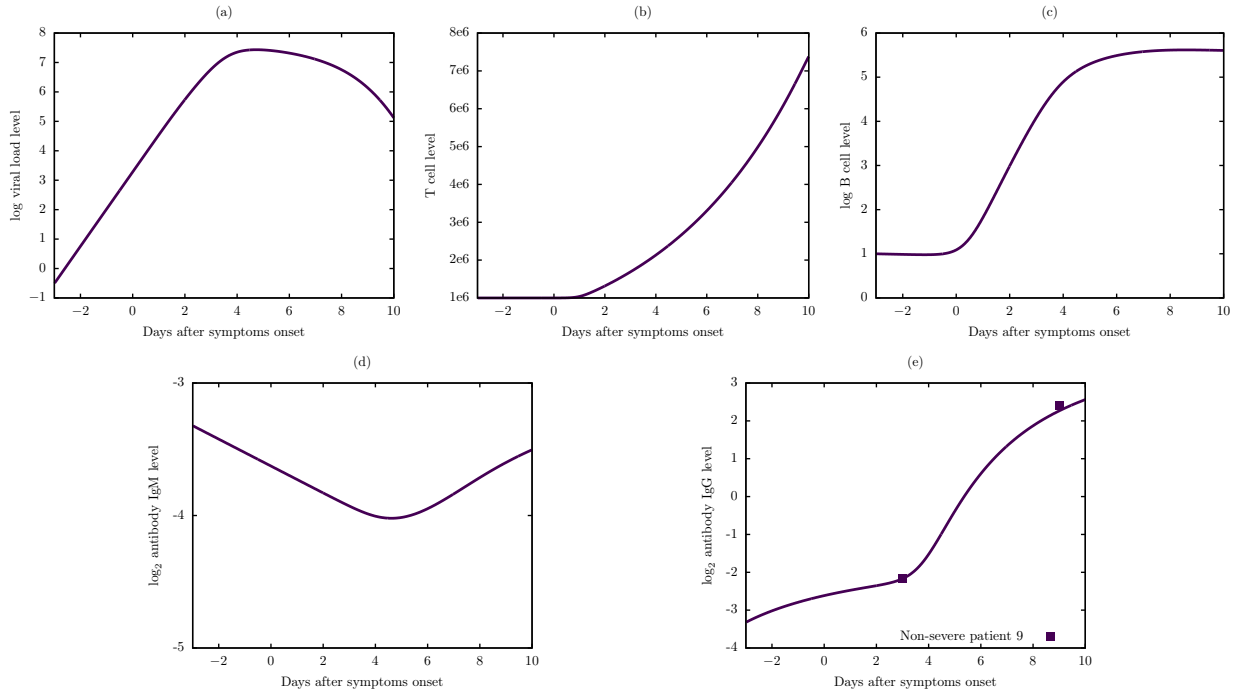


Figure S13: Viral dynamic and immune response of Model 6 for non-severe patient 9.

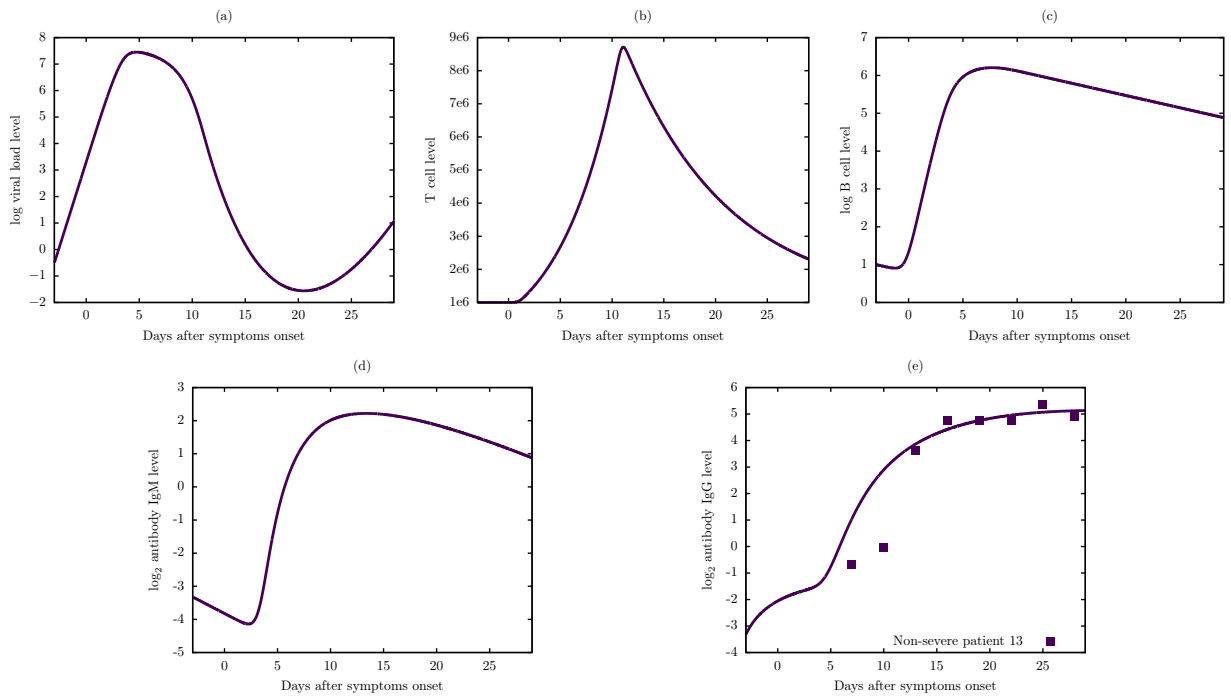


Figure S14: Viral dynamic and immune response of Model 6 for non-severe patient 13.

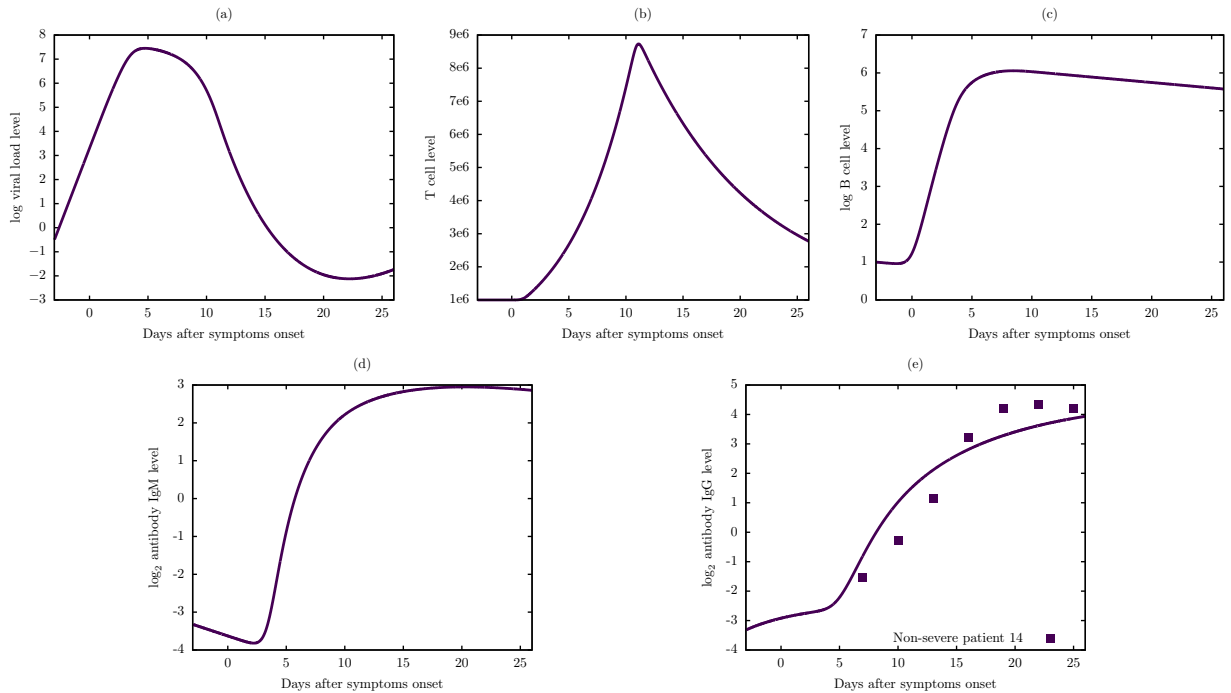


Figure S15: Viral dynamic and immune response of Model 6 for non-severe patient 14.

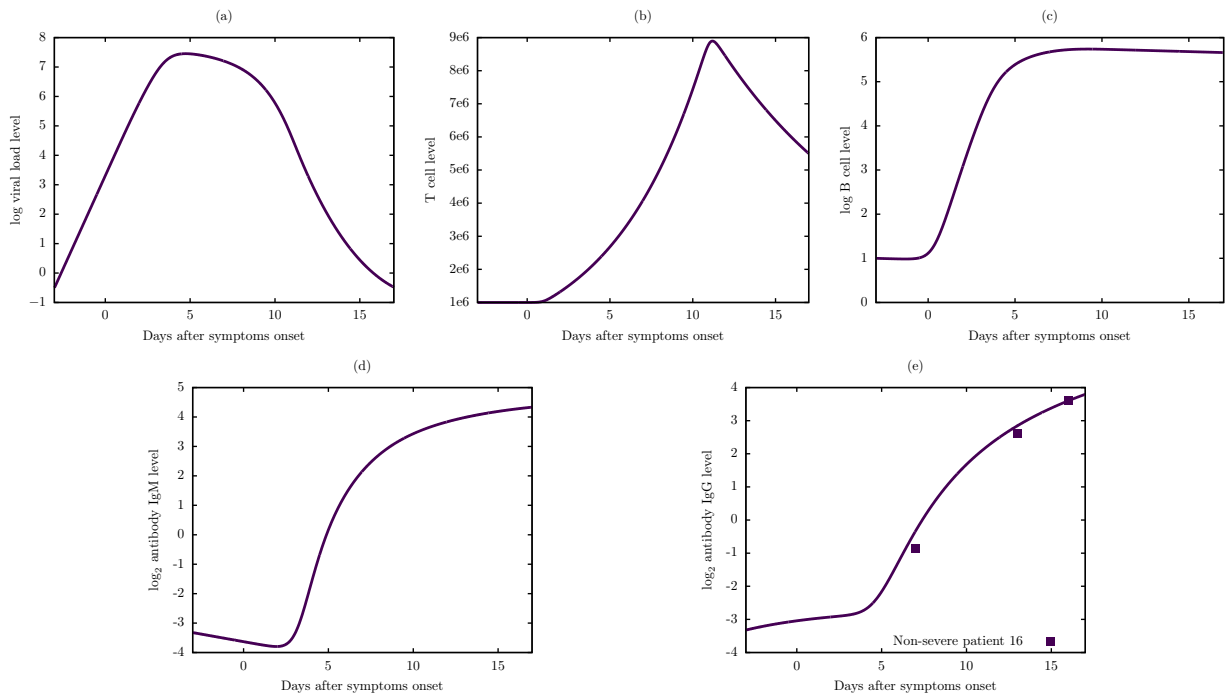


Figure S16: Viral dynamic and immune response of Model 6 for non-severe patient 16.

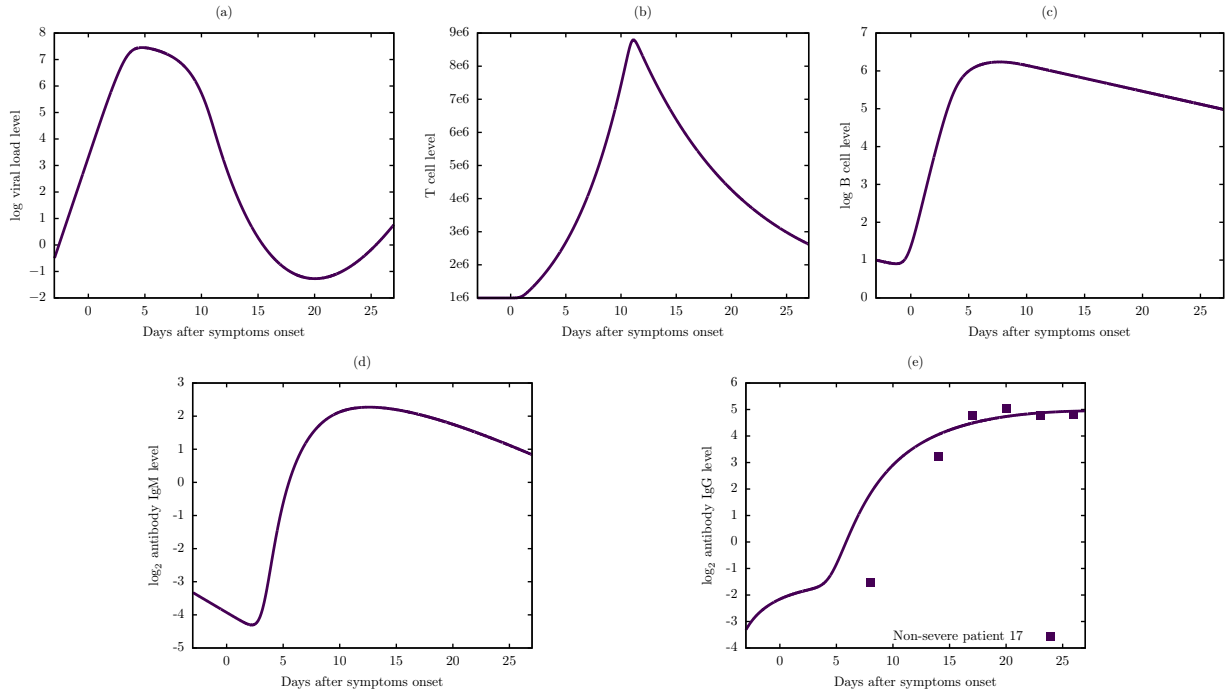


Figure S17: Viral dynamic and immune response of Model 6 for non-severe patient 17.

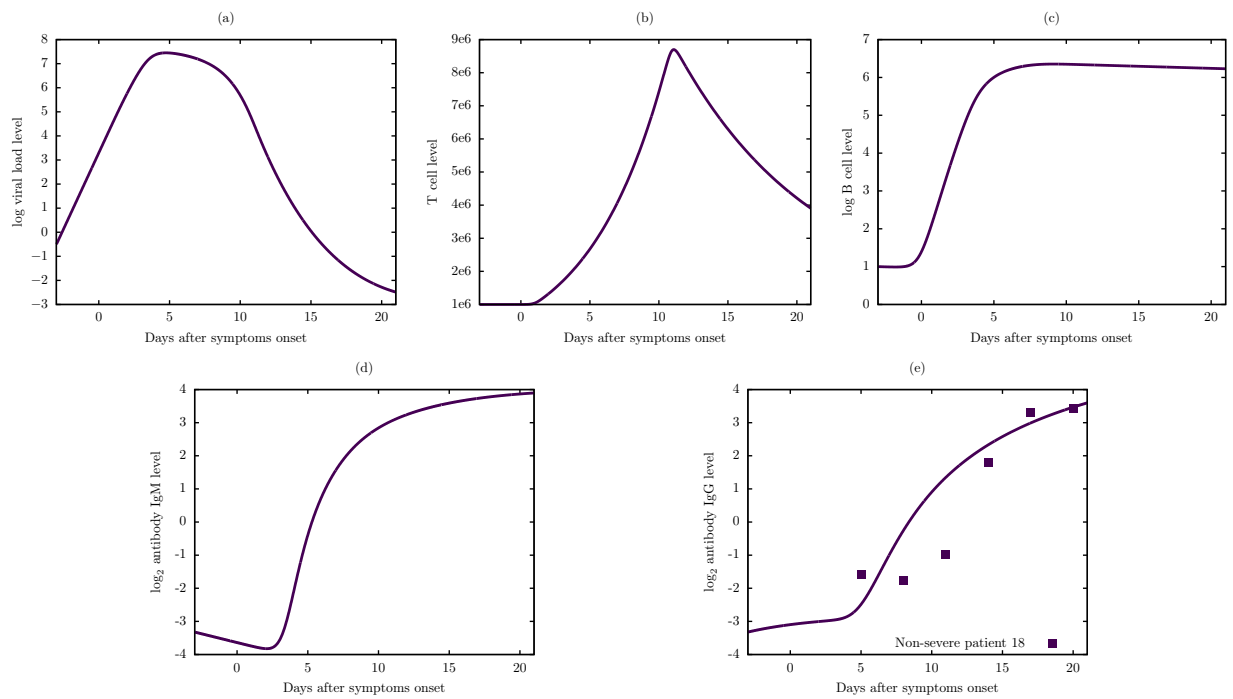


Figure S18: Viral dynamic and immune response of Model 6 for non-severe patient 18.

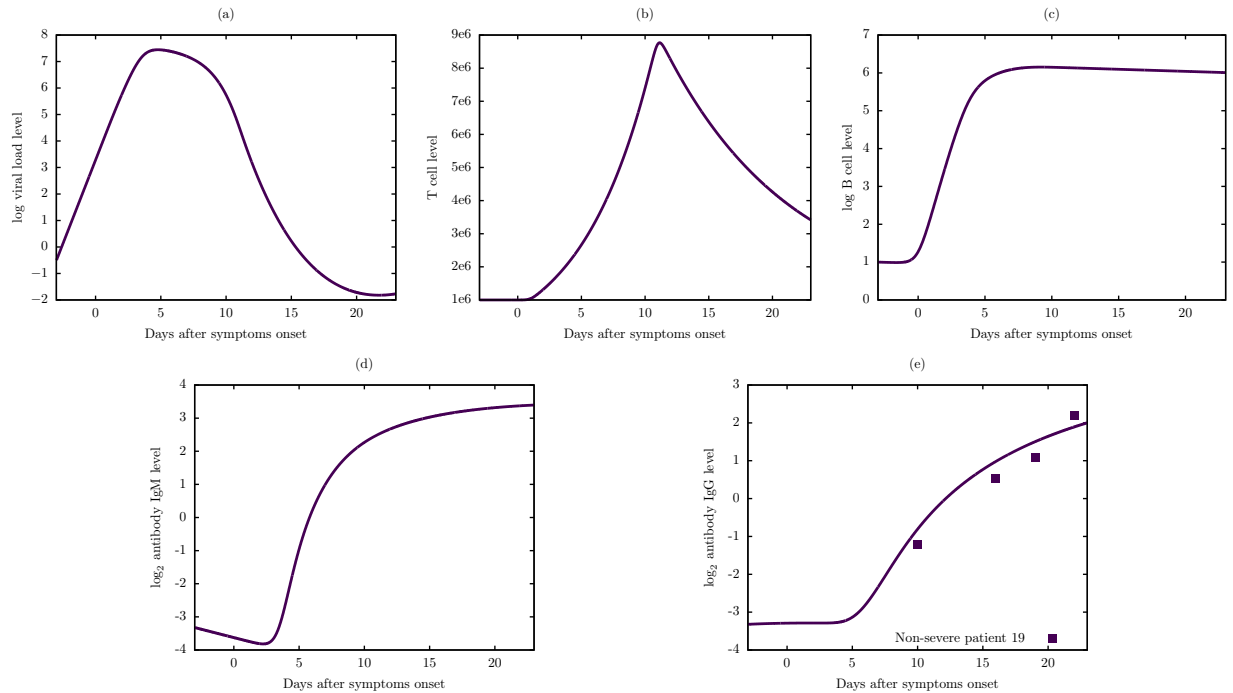


Figure S19: Viral dynamic and immune response of Model 6 for non-severe patient 19.

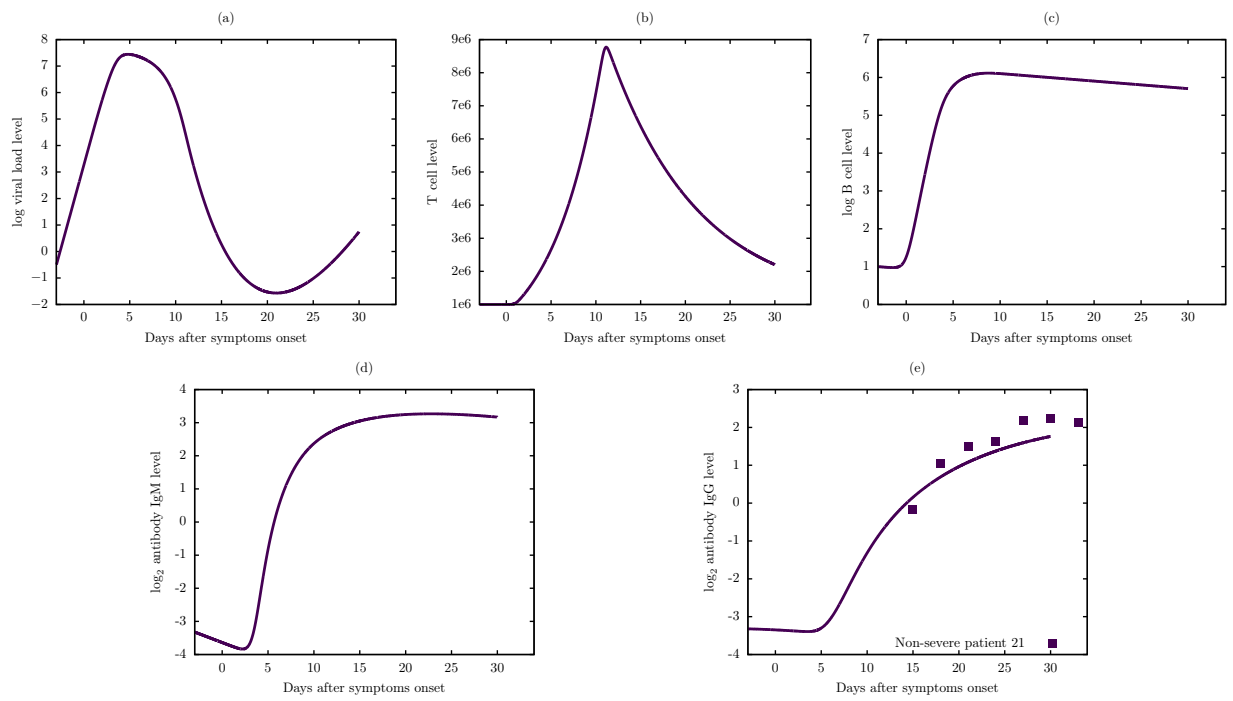


Figure S20: Viral dynamic and immune response of Model 6 for non-severe patient 21.

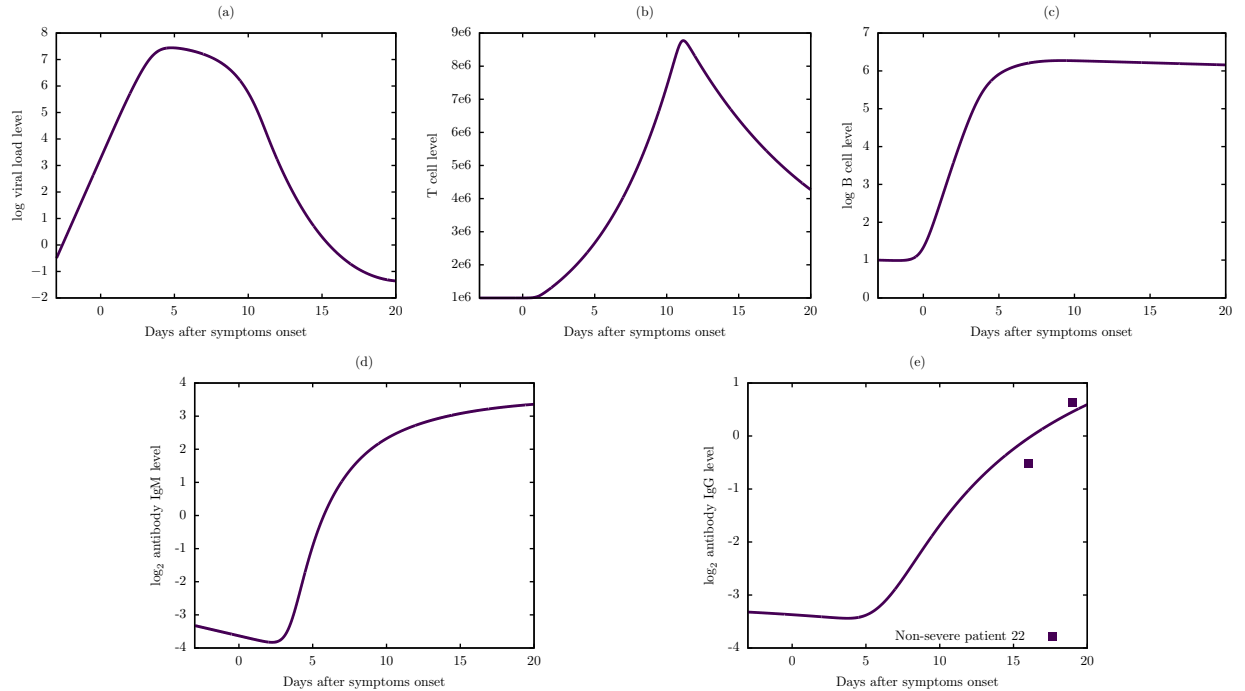


Figure S21: Viral dynamic and immune response of Model 6 for non-severe patient 22.

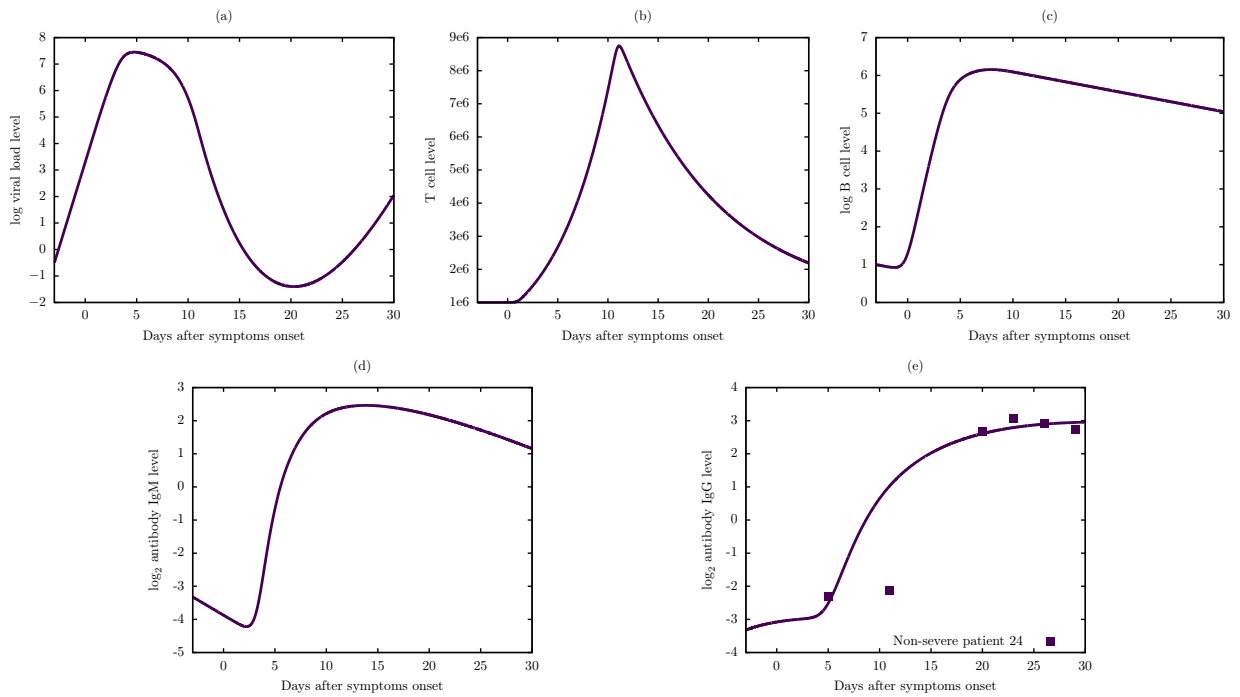


Figure S22: Viral dynamic and immune response of Model 6 for non-severe patient 24.

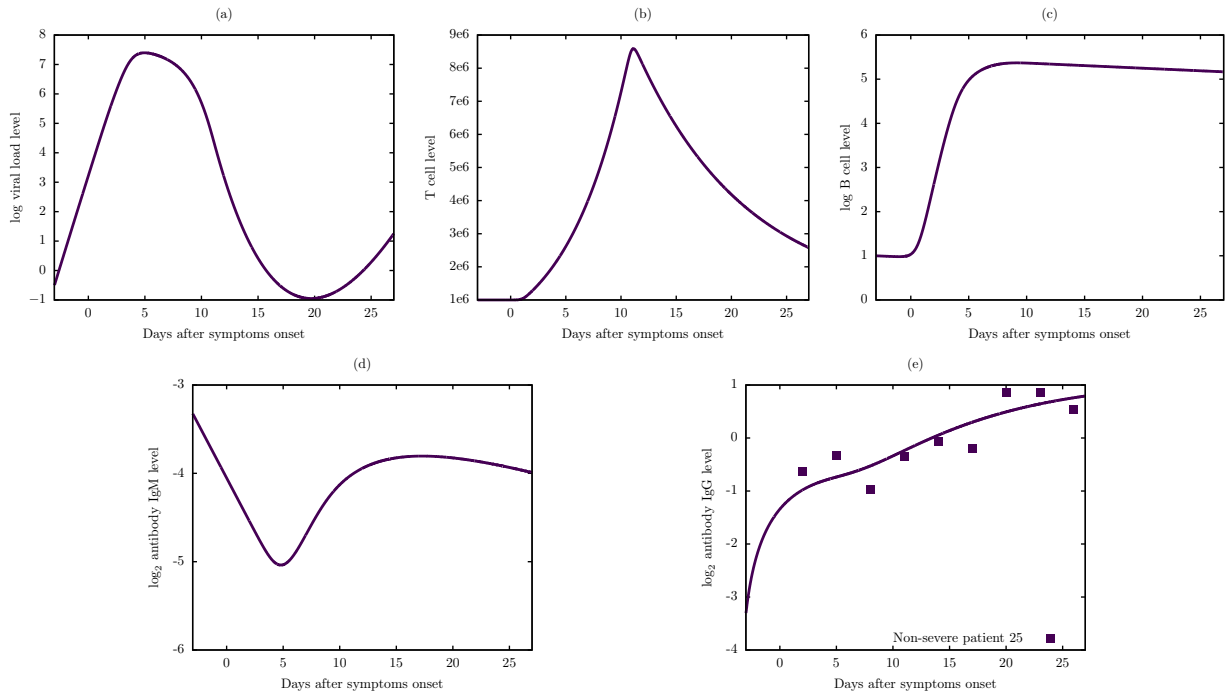


Figure S23: Viral dynamic and immune response of Model 6 for non-severe patient 25.

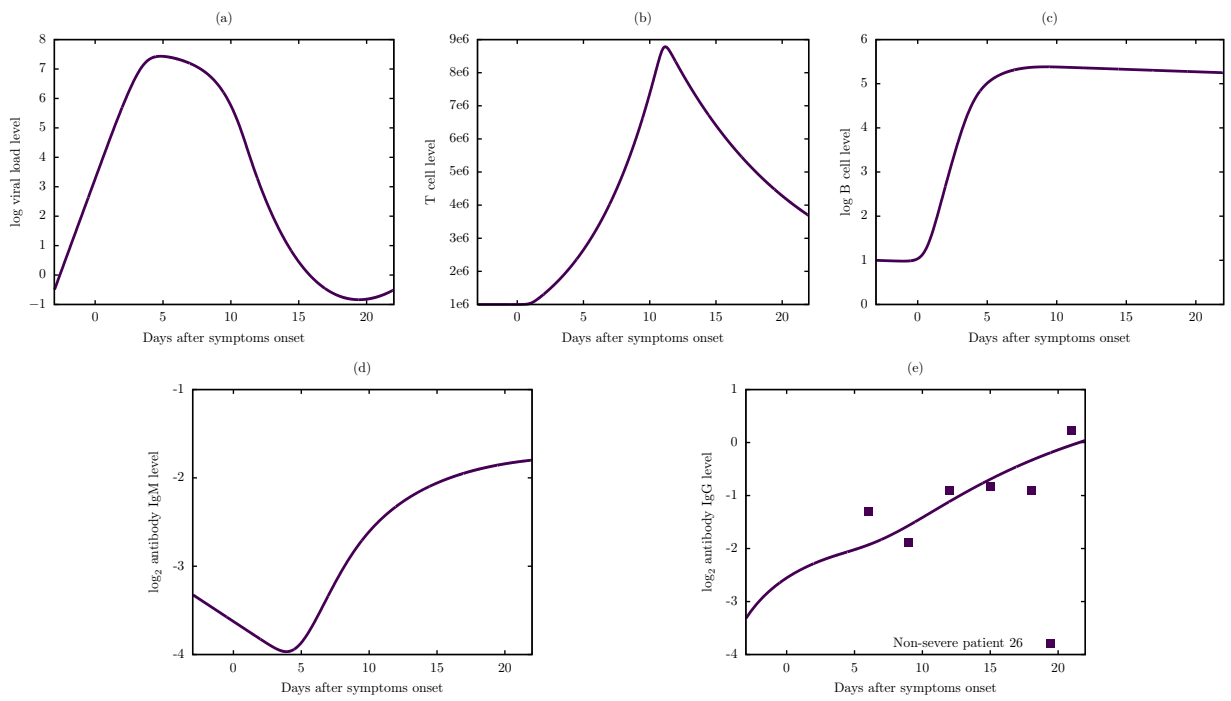


Figure S24: Viral dynamic and immune response of Model 6 for non-severe patient 26.

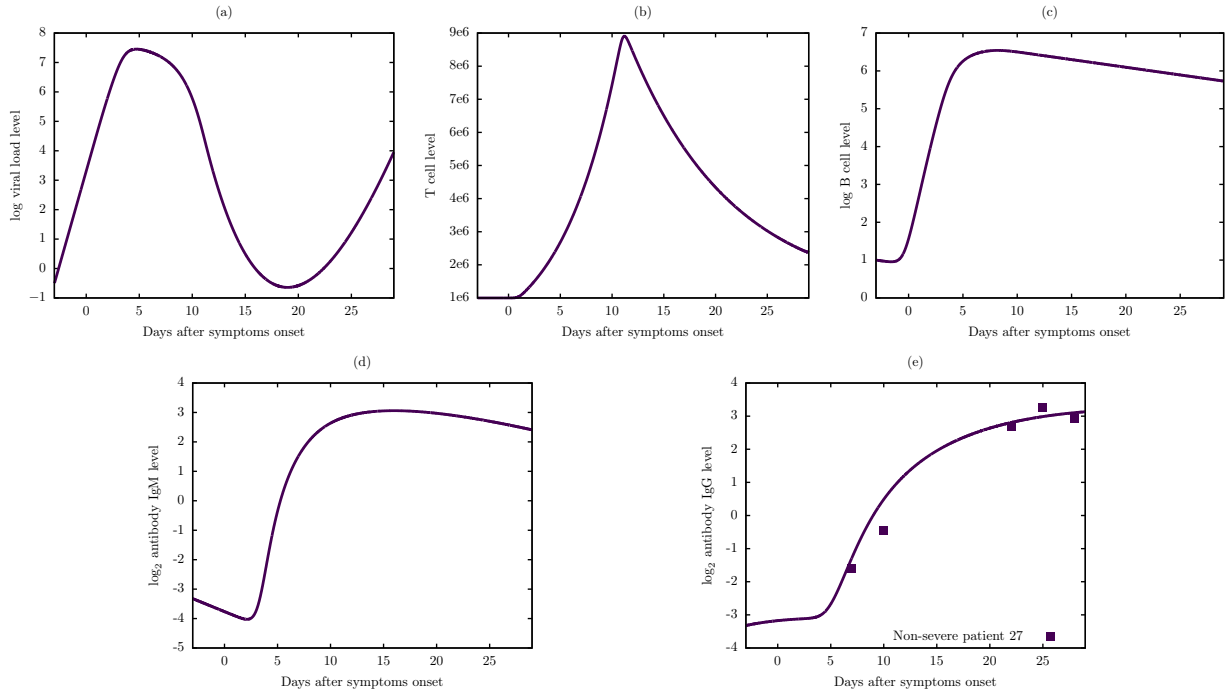


Figure S25: Viral dynamic and immune response of Model 6 for non-severe patient 27.

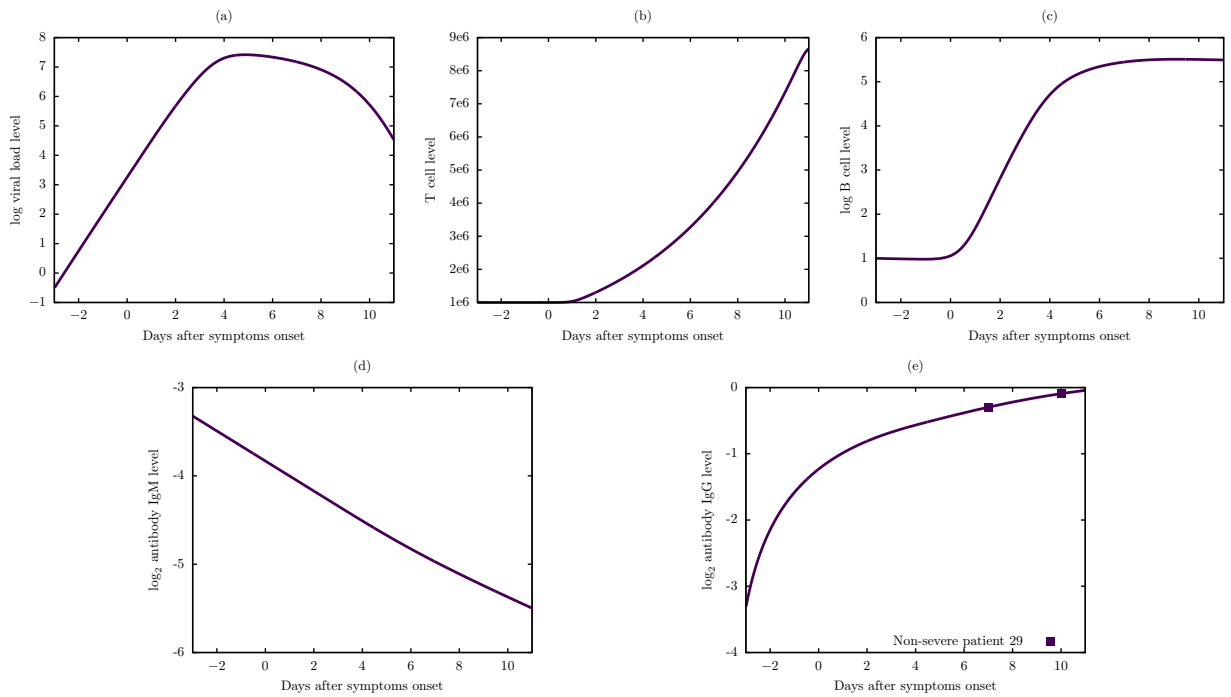


Figure S26: Viral dynamic and immune response of Model 6 for non-severe patient 29.

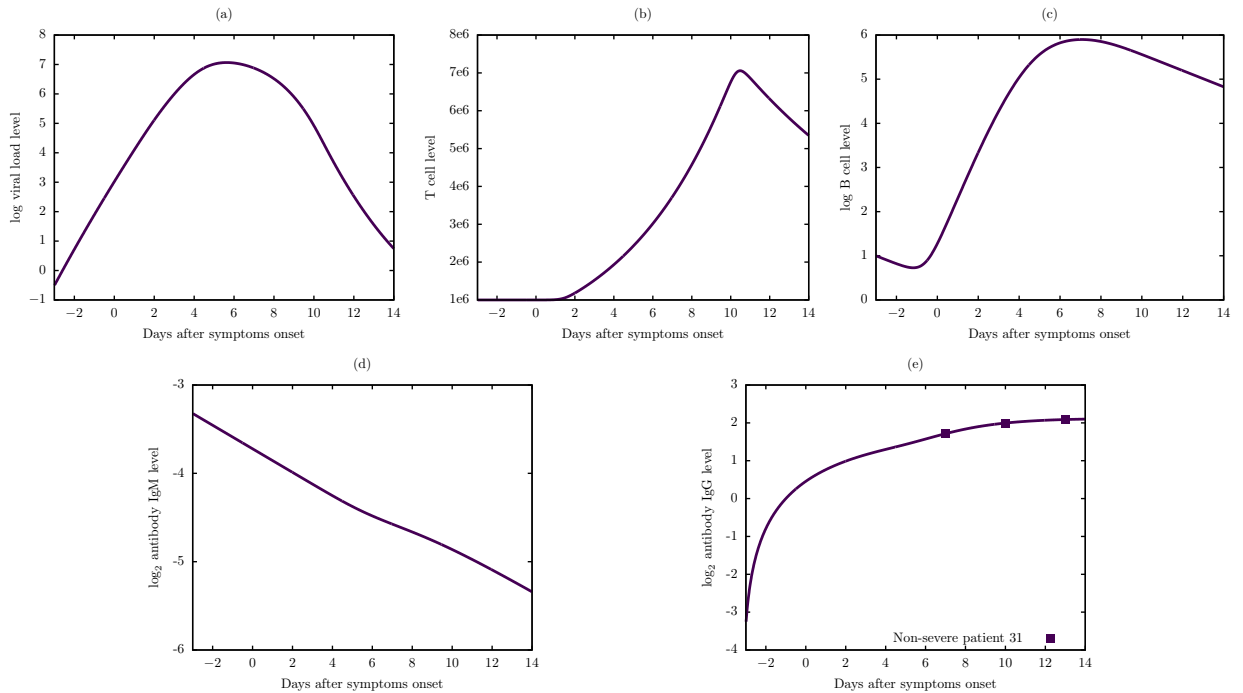


Figure S27: Viral dynamic and immune response of Model 6 for non-severe patient 31.

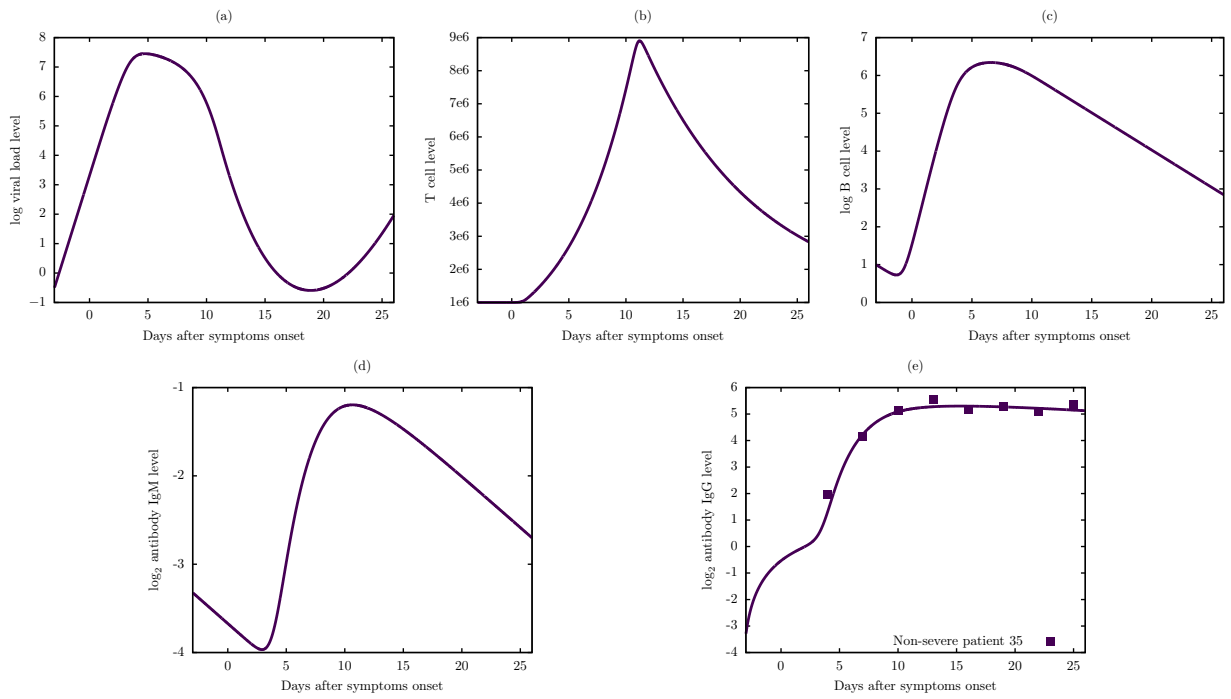


Figure S28: Viral dynamic and immune response of Model 6 for non-severe patient 35.

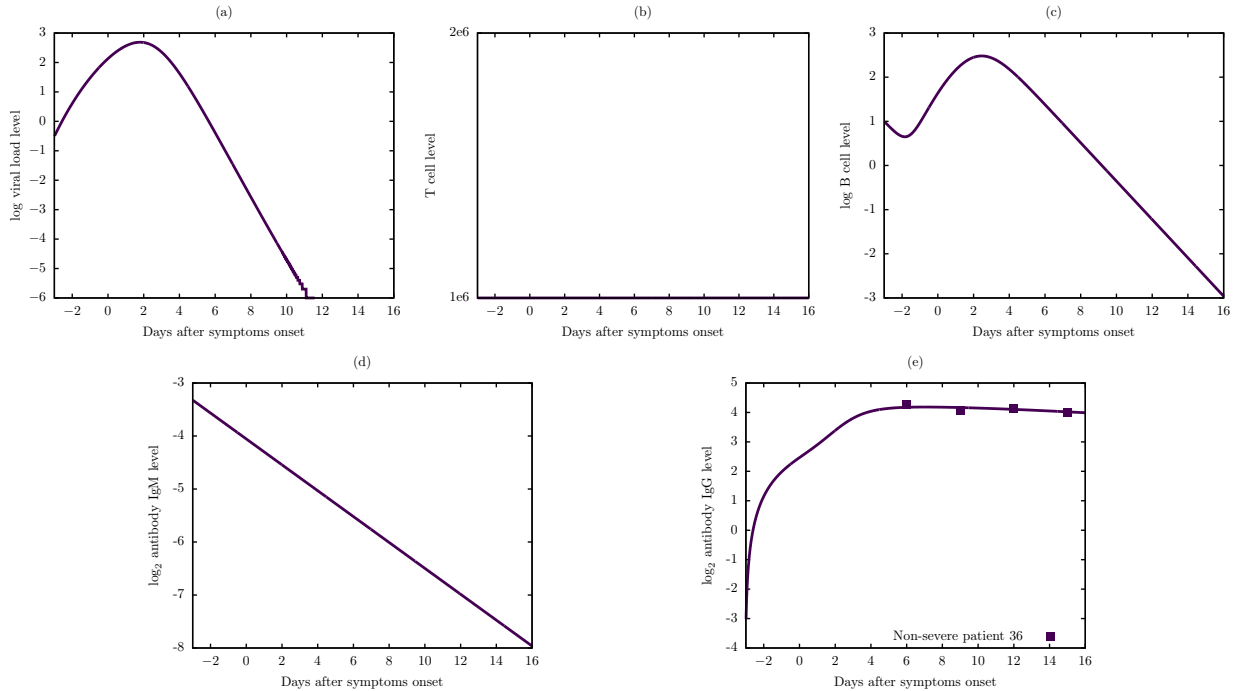


Figure S29: Viral dynamic and immune response of Model 6 for non-severe patient 36.

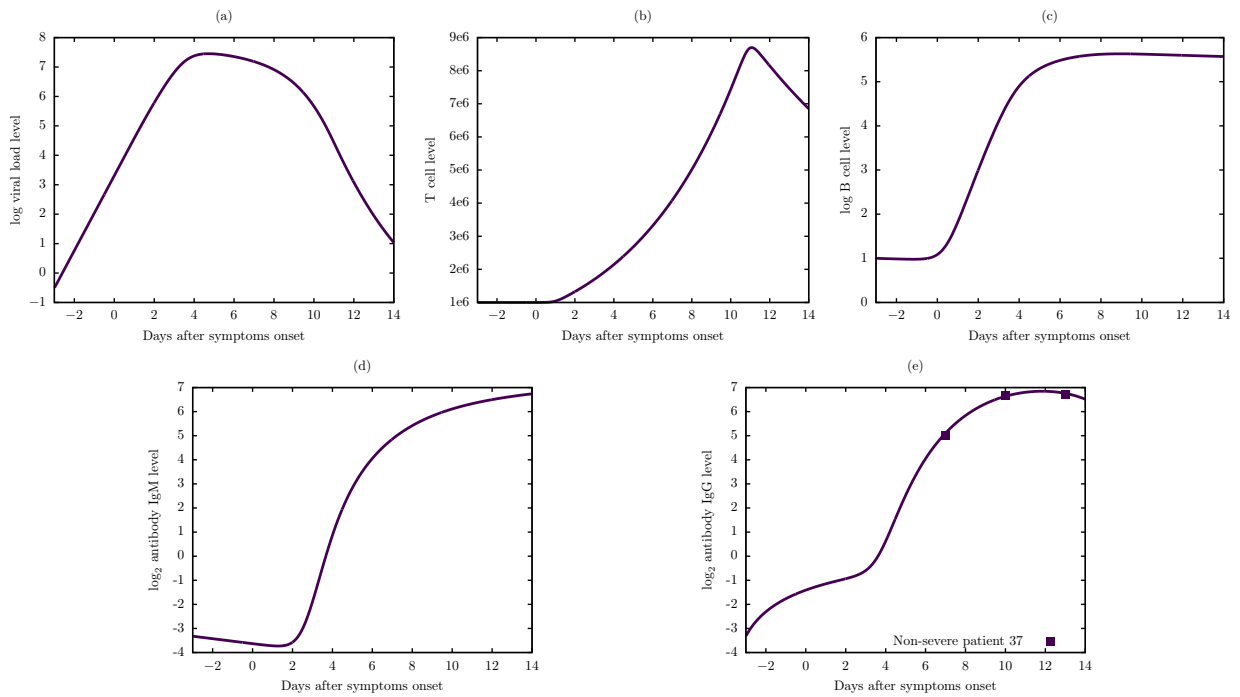


Figure S30: Viral dynamic and immune response of Model 6 for non-severe patient 37.

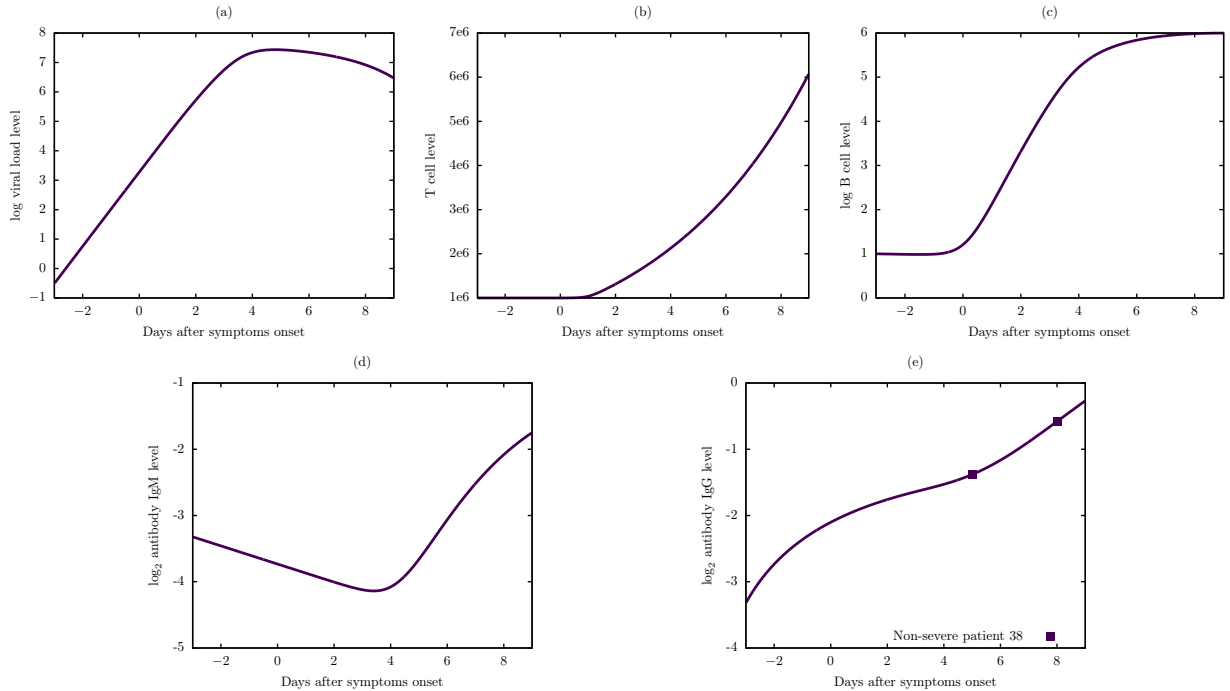


Figure S31: Viral dynamic and immune response of Model 6 for non-severe patient 38.

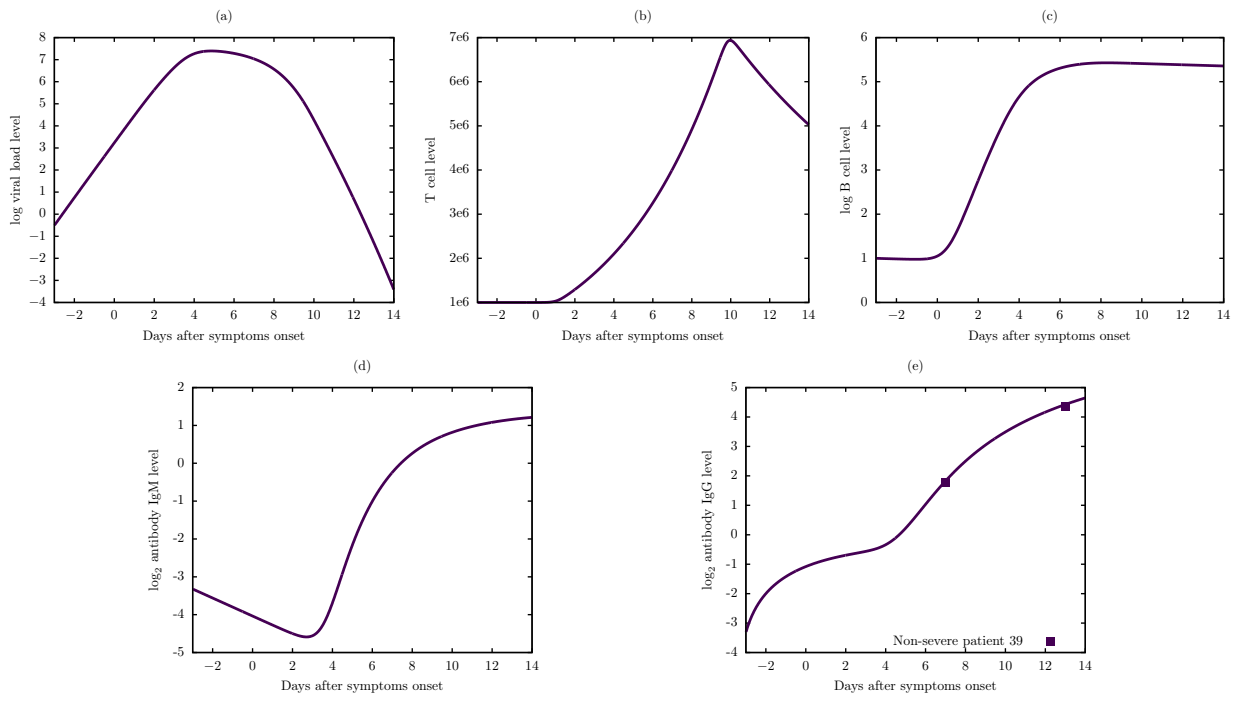


Figure S32: Viral dynamic and immune response of Model 6 for non-severe patient 39.

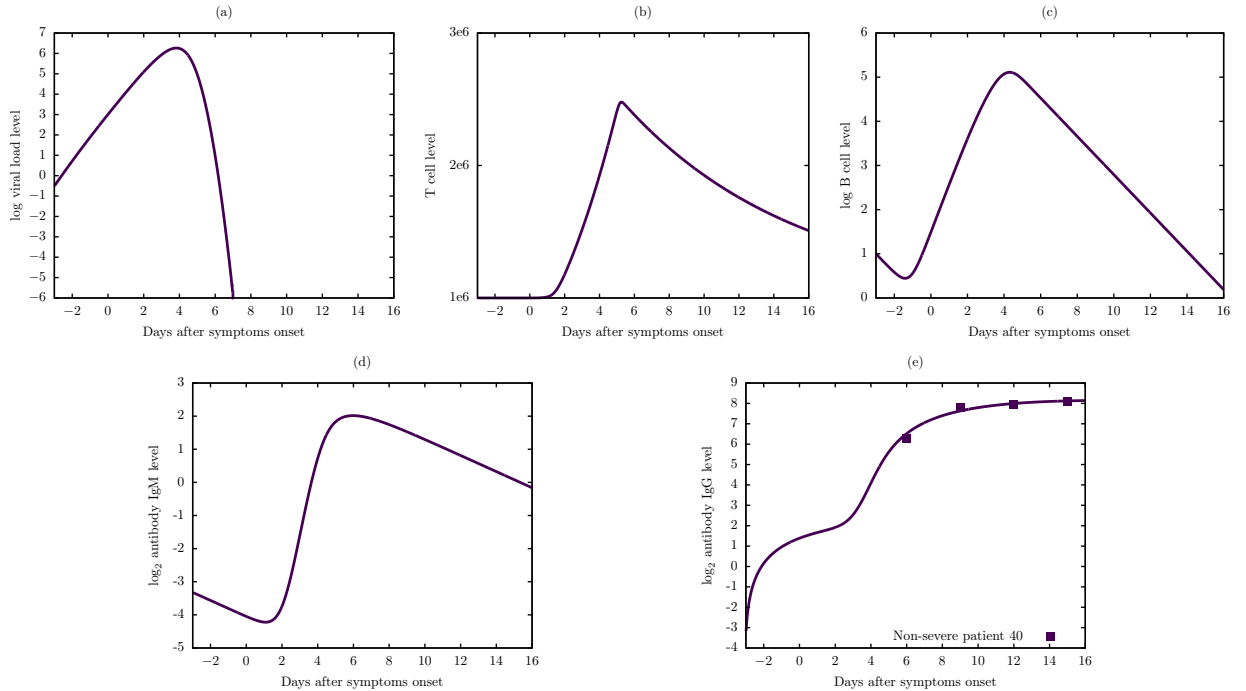


Figure S33: Viral dynamic and immune response of Model 6 for non-severe patient 40.

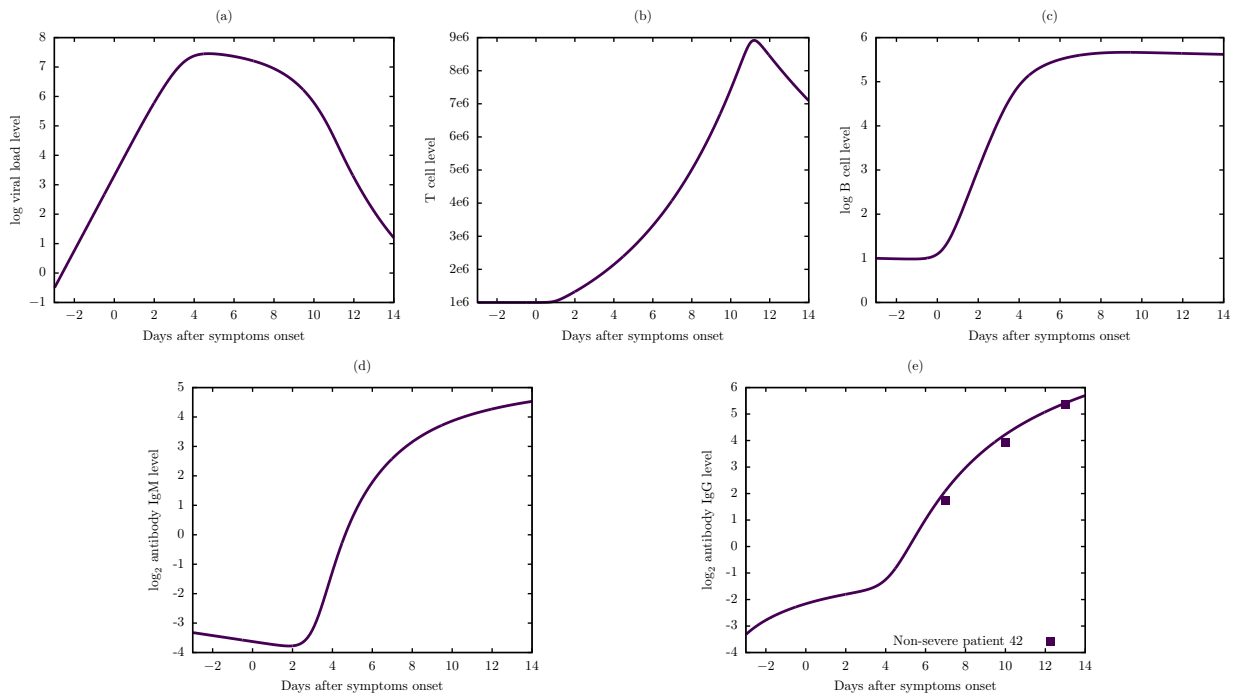


Figure S34: Viral dynamic and immune response of Model 6 for non-severe patient 42.

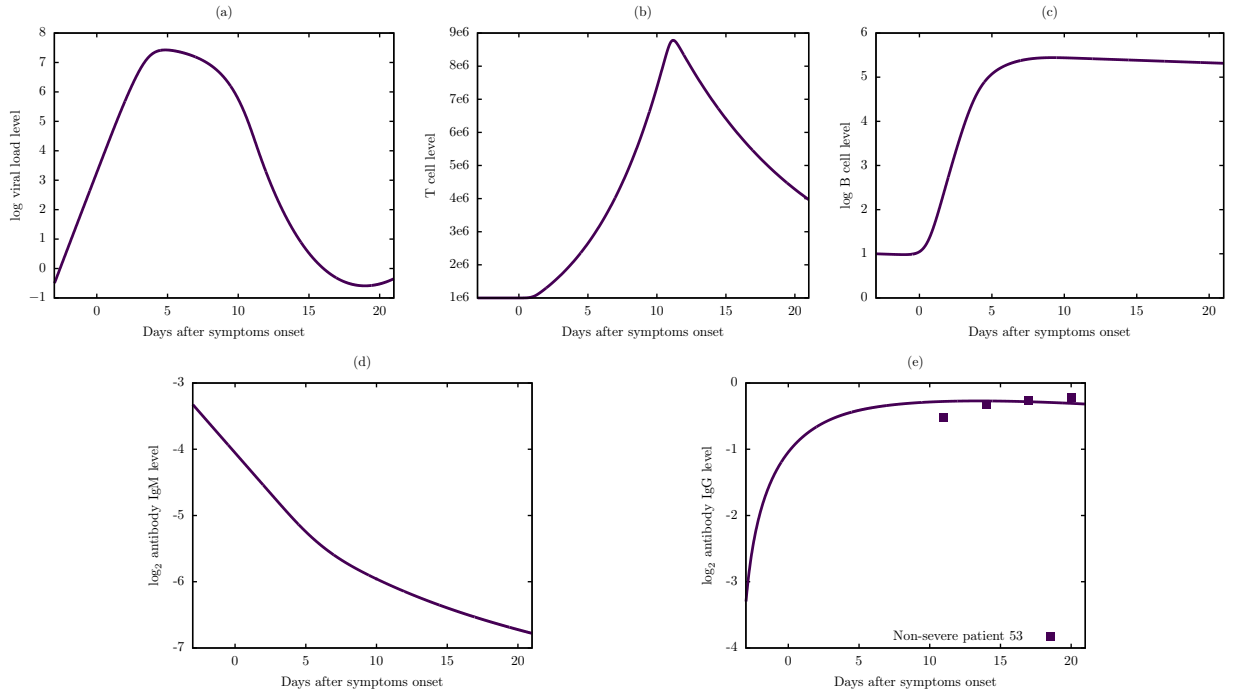


Figure S35: Viral dynamic and immune response of Model 6 for non-severe patient 53.

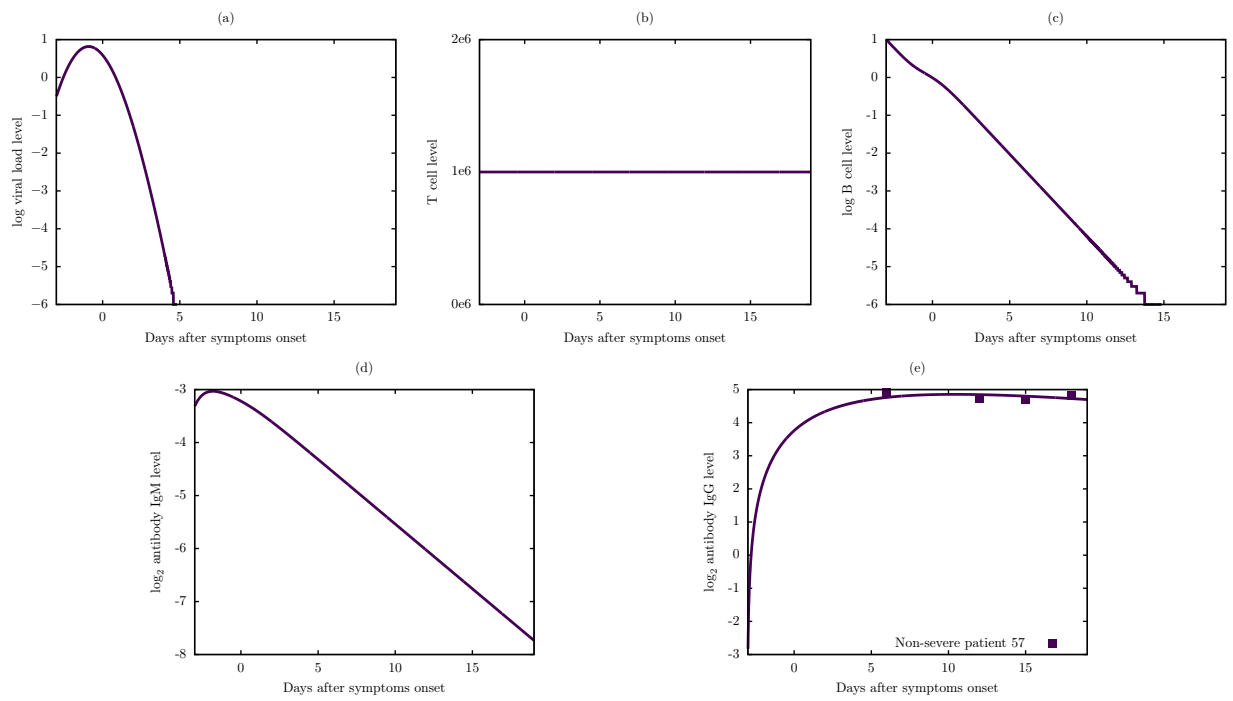


Figure S36: Viral dynamic and immune response of Model 6 for non-severe patient 57.

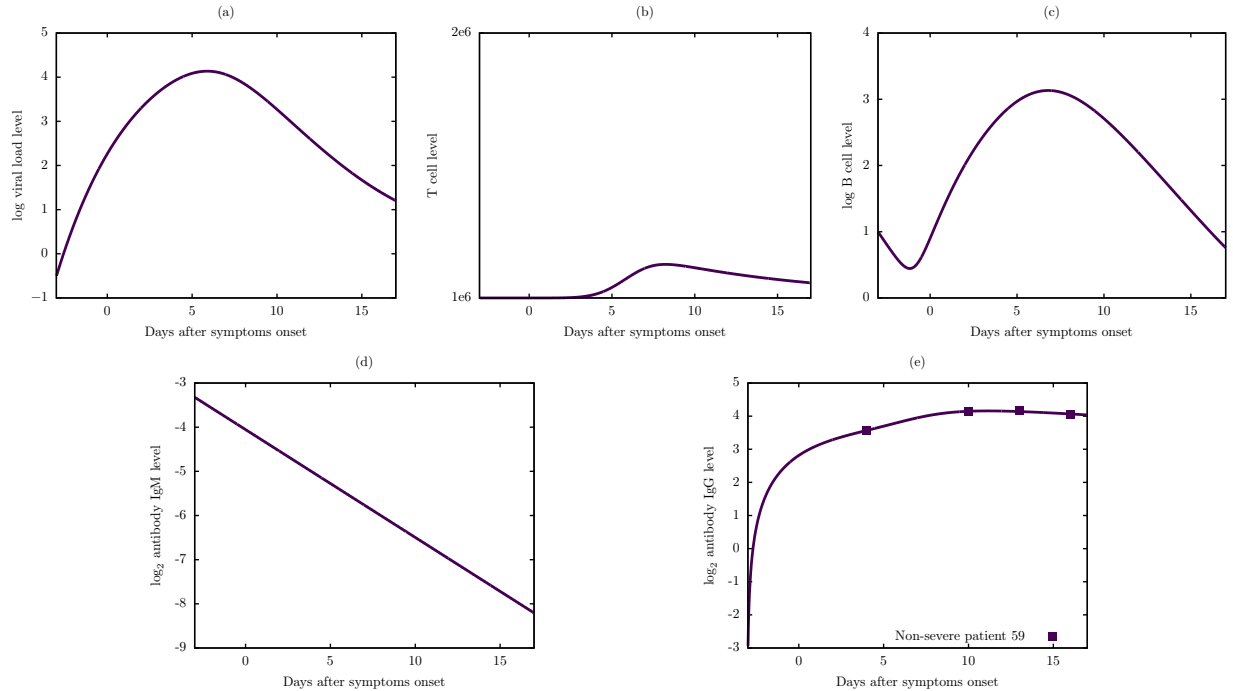


Figure S37: Viral dynamic and immune response of Model 6 for non-severe patient 59.

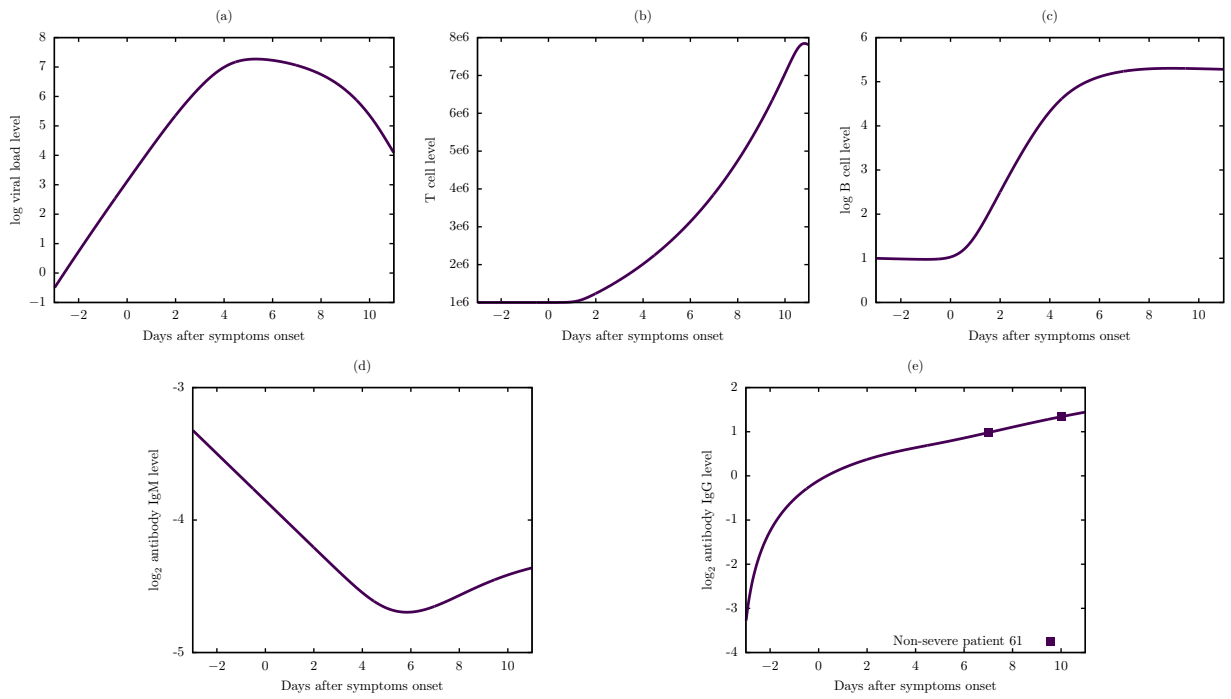


Figure S38: Viral dynamic and immune response of Model 6 for non-severe patient 61.

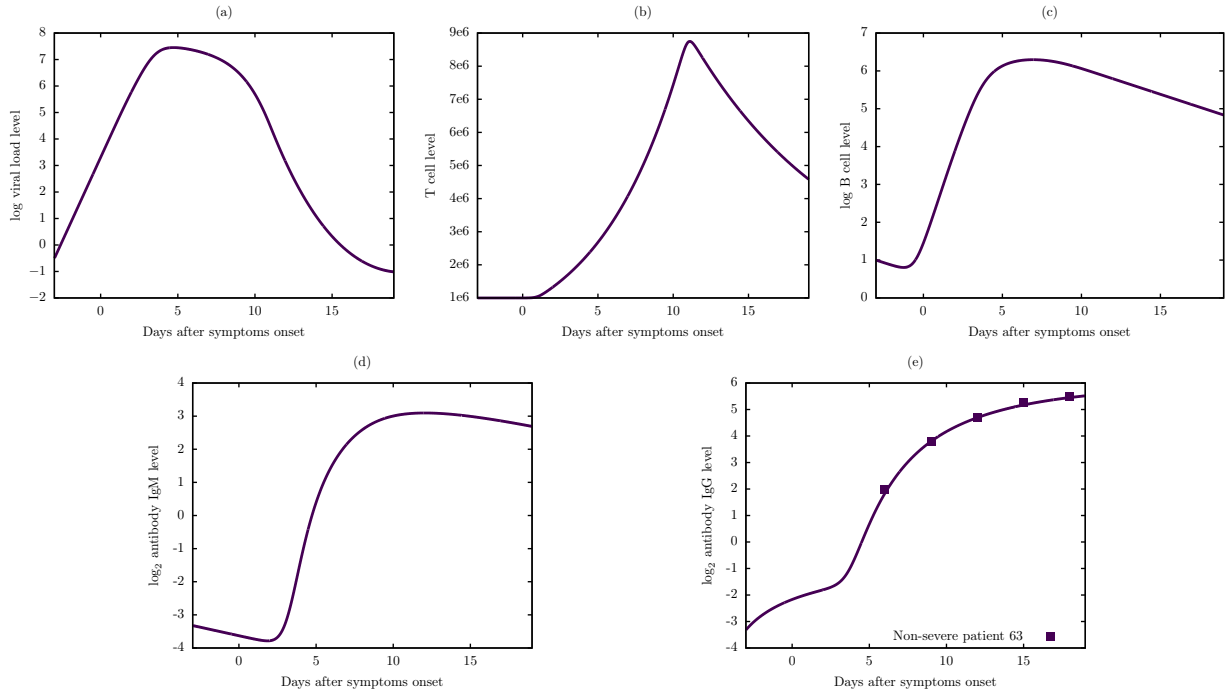


Figure S39: Viral dynamic and immune response of Model 6 for non-severe patient 63.

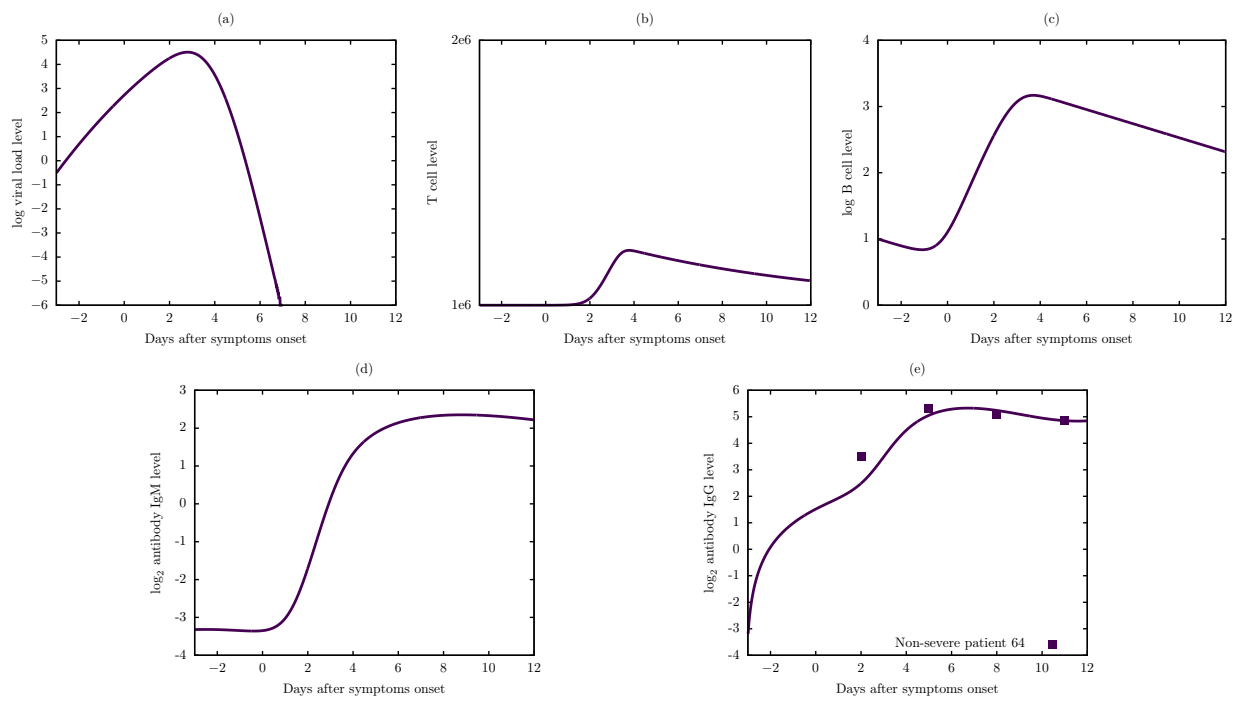


Figure S40: Viral dynamic and immune response of Model 6 for non-severe patient 64.